Reviews on Advanced Materials and Technologies, 2024, vol. 6, no. 3, pp. 132–156
DOI: 10.17586/2687-0568-2024-6-3-132-156

Stresses in Local Volumes During Reactive Sintering of Powder Mixture Ti-Al-Fe-Fe_2O_3

A.G. Knyazeva*, M.A. Anisimova

Institute of Strength Physics and Materials Science SB RAS, pr. Academicheskii, 2/4, Tomsk, Russia

Article history

Received September 21, 2024
Accepted September 28, 2024
Available online September 30, 2024

Abstract

Composites based on titanium and aluminium have been attracting attention for decades. One of the possible ways of creating such composites is based on reaction sintering, which implies sintering with accompanying chemical reactions, the consequence of which is a change in phase composition. The number of reactions may directly include those that lead to the formation of the hardening phase. Mixtures of the Ti-Al-Fe-Fe_2O_3 type, where the source of iron oxide is metalworking waste, are very promising for use in this direction. However, for multicomponent systems the regularities of phase formation, as well as the appearance of stresses in the diffusion zone, are not obvious and are not the same for the entire volume of reaction mixtures. The present paper describes general ideas and methods of modelling for reactive sintering and gives an overview of the situations that are most important for phase formation in a selected mixture. It is shown that the dynamics of phase growth and stresses can be different in different local volumes with various variants of particles meeting each other.

Keywords: Reactive diffusion; Phase growth; Stresses

1. INTRODUCTION

Composites based on titanium and aluminium are used in various industries due to a good combination of important properties: relatively low density, high strength and corrosion resistance. Additional components are widely used both in the form of simple elements and in the form of chemical compounds (oxides, borides, carbides, silicides), which significantly increase functional, physical and mechanical characteristics of titanium-based alloys. One of the possible options for creating composites is the use of reaction sintering, during which the strengthening phase in the form of oxides is directly synthesised. For example, in the system Ti+Al+Fe+Fe_2O_3, depending on the percentage of powders, the homogeneity of mixing and the nature of heating, it is possible to identify different variants of meso-volumes, in which the sequence of reactions and accompanying phenomena can lead to different phase composition. As a result, the composition of the whole composite will be very heterogeneous. In order to analyse possible variants of development of events in the conditions of reaction sintering on the basis of literature data in Refs. [1,2], specific variants of particles meeting with each other and variants of phase formation under changing temperature conditions were analysed. The systems Ti+Al (reactions take place in the melt) and Ti+Al (interaction takes place in the solid phase in a diffusion pair at constant temperature); three variants of interphase interaction are distinguished: Ti (melt)+Fe_2O_3 (solid); Al (melt)+Fe_2O_3 (solid); (Ti+Al) (melt)+Fe_2O_3 (solid). At equilibrium synthesis of materials from binary powder mixtures at the interface of interacting components the so-called diffusion zone is formed, which, as a rule, is multilayer (multiphase) and is largely determined by the processes of mutual diffusion in the phases. In nonequilibrium conditions and in multicomponent systems kinetic regularities are not obvious and are different in different local volumes.

In the present paper, an overview of the basic concepts of phase growth in the diffusion zone is given (Section 2.1) and examples of works in which the stresses accompanying

* Corresponding author: A.G. Knyazeva, e-mail: anna-knyazeva@mail.ru

phase formation are evaluated are given (Section 2.2). Further, within the framework of the theory of reactive diffusion, the main situations leading to inhomogeneous phase composition are described (Section 3.1) and a comparison of the magnitudes and distributions of stresses in regions containing mobile phase-separation boundaries is given (Section 3.2). In fact, Section 3 of the paper presents a small review of the authors' work on the theoretical study of phase formation in the system under reaction sintering conditions.

2. THE SIMPLEST IDEAS ABOUT PHASE GROWTH IN THE DIFFUSION ZONE AND ASSOCIATED STRESSES

2.1. Problems of the reactive diffusion theory

The term ‘reactive sintering’ is defined in Ref. [3] as solid-phase sintering of multicomponent systems accompanied by the interaction of components and the formation of chemical compounds. However, reactive sintering can also occur in the presence of a liquid phase, which significantly facilitates the interaction of components. In both cases, solid phases participate in chemical reactions that leads to the necessity to consider diffusion as a full-valid stage of chemical reactions.

In diffusion theory there are several different concepts [4], which are directly relevant to modelling the production of new materials. Diffusion of foreign atoms in a material is called heterodiffusion, in contrast to self-diffusion, which occurs in the absence of a chemical potential gradient. Chemical diffusion [5] (diffusion in substances of variable composition; diffusion under the action of a chemical composition gradient) and reactive diffusion [6] (diffusion together with a chemical reaction) are often used as practically identical concepts. Further we will understand by chemical diffusion the diffusion in one phase, and by reactive diffusion—diffusion in a system with several phases, the ratio between which changes. Problems of reactive diffusion occur in different sections of materials science and are directly related to the formation of composition in the synthesis of new materials, the evolution of composition in different processes of surface treatment and corrosion of materials and coatings in a chemically active medium. When formulating the corresponding problems, it is taken into account that the stages limiting the rates of chemical reactions are diffusion processes [6–8]. The term ‘Multiphase diffusion’ is encountered in the English-language literature, which implies diffusion leading to the formation of a new interface, new phases, solid solutions and/or chemical compounds, i.e., we are also talking about reactive diffusion.

One of the first models of the theory of reactive diffusion is considered to be the Wagner oxidation model, which takes into account the reaction on the outer surface of the growing oxide film, the reaction on its inner surface, and the diffusion of ions to each other through this layer. Similar models take place for other diffusion-controlled reactions. The simplest problem on the growth of a single-layer oxide film on a metal surface in neglecting the solubility of oxygen in the metal can be formulated as follows:

$$\frac{\partial C}{\partial t} = \frac{\partial}{\partial x}\left(D\frac{\partial C}{\partial x}\right);$$

$$C(0,t) = C_1,\ C(\xi,t) = C_2,\ C(x>\xi,t) = 0;$$

$$x = \xi:\ -D\frac{\partial C}{\partial x} = C_2\frac{d\xi}{dt}.$$

At the initial point in time, there is only the starting material. The last relation is a mass balance and follows from the condition that all diffusant supplied to the growing phase through the surface $x = \xi$ above the concentration C_2, goes to the formation of a new phase.

Two simple methods are popular for the analytical solution of such problems. In one of them the solution is sought in the form

$$C = A + B\,\Phi(z),$$

where

$$\Phi(z) = \operatorname{erf}(z) = \frac{2}{\sqrt{\pi}}\int_0^z \exp\left(-y^2\right)dy,\ z = \frac{x}{2\sqrt{Dt}}.$$

The distribution of concentrations has the form

$$C = C_1 + \frac{C_2 - C_1}{\Phi\left(\dfrac{\xi}{2\sqrt{Dt}}\right)}\Phi\left(\frac{x}{2\sqrt{Dt}}\right).$$

Since the solution must be true at any point in time, including the initial one, we must take

$$\xi = 2a\sqrt{Dt}.$$

Hence, the condition for the flux gives a transcendental equation for finding the constant a

$$\frac{C_1 - C_2}{C_2} = a\sqrt{\pi}\Phi(a)\exp\left(a^2\right) \tag{1}$$

and concentration distribution

$$C = C_1 + \frac{C_2 - C_1}{\operatorname{erf}(a)}\Phi\left(\frac{x}{2\sqrt{Dt}}\right). \tag{2}$$

For small a we obtain from Eq. (2):

$$a = \sqrt{\frac{C_1 - C_2}{2C_2}}. \tag{3}$$

In this case

$$\xi = 2a\sqrt{Dt} \approx 2\sqrt{D\frac{C_1 - C_2}{2C_2}t}\,. \qquad (4)$$

Another way of determining the growth law of the new phase is reduced to the quasi-stationary approximation, which, by definition, does not work at small times, actually corresponding to the stage of formation of a continuous interface between the new and old phases. In this method, the distribution of concentrations between surfaces $x = 0$ and $x = \xi$ follows from the stationary equation

$$\frac{d}{dx}\left(D\frac{dC}{dx}\right) = 0$$

and has the form

$$C = C_1 + (C_2 - C_1)\frac{x}{\xi}\,. \qquad (5)$$

The law of motion of the boundary follows from mass balance:

$$\xi = \sqrt{2D\frac{C_1 - C_2}{C_2}t}\,.$$

This formula coincides with Eq. (4).

However, if the condition of smallness of the parameter a is not fulfilled, the difference in the results obtained by different methods can be significant. This is illustrated by Figs. 1 and 2, for which $a \to 1$. Both methods give a parabolic growth law. However, by the same point in time, shown by the dashed vertical line in Fig.1, the sizes of the oxide phases are significantly different (Fig. 2a). The concentration distributions in the phases are also different (Figs. 2a,b).

If in this simple model we take into account the diffusion into the basic material, the condition at the moving boundary will take the form

$$x = \xi(t):\ [\mathbf{J}_2 - \mathbf{J}_{Me}] = [C_2 - C_{Me}]\frac{d\xi}{dt}, \qquad (6)$$

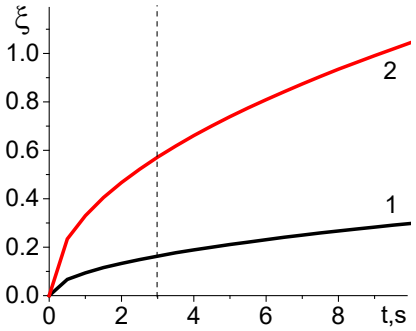

Fig. 1. Change in the position of the interphase boundary with time in the example of Al_2O_3 phase growth. 1 – first method, 2 – second method. $C_1 = 0.8$, $C_2 = 0.01$, $T = 1000$ K, $D = 6.9 \cdot 10^{-4}$ μm²/s.

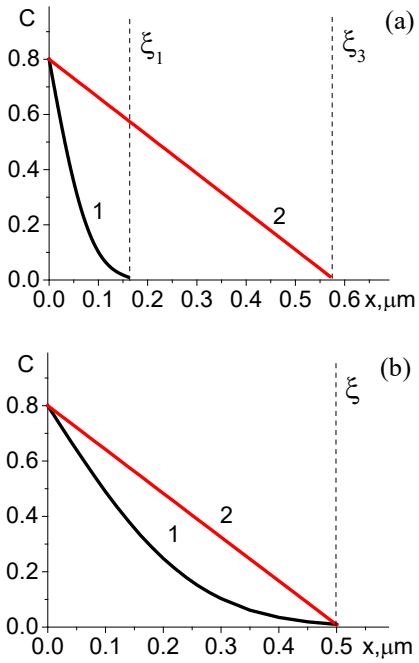

Fig. 2. Concentration distribution in the region of the new phase (Al_2O_3) at the time $t = 3$ s (a) and in transient layer of the same thickness (b).

where $\mathbf{J}_{Me} = -D_{Me}(\partial C/\partial x)$ is the diffusant flow on the metal side; $\mathbf{J}_2 = -D_2(\partial C/\partial x)$ is the diffusant flux from the growing phase side.

Note, that both methods are approximate as well as the problem statements of theory of reactive diffusion themselves.

Similar problems, taking into account various coupled effects, are applied to the processes of chemical-thermal treatment, welding, coating and others. The theory is easily generalised to samples of spherical and cylindrical shapes, including the interaction of metals with gases [9,10]; to the description of the growth of several layers [11]. However, the simultaneous appearance and further growth of more than two layers of new phases in binary systems [6] is rather an exception than a rule. Attempts of generalisation to the processes of phase growth in the presence of defects and different variants of defect formation are known [12,13]. However, the parabolic growth law is not always fulfilled, which is due to both geometrical factors and competing processes of phase formation. In complex media, kinetic features of phase formation are associated with the presence of cross diffusion fluxes; with the influence of defects, mechanical stresses and electromagnetic fields on diffusion [5,14,15]. It is known that bulk diffusion is not necessarily the process controlling the rate of reactive diffusion for all alloy systems. The unification of the theories of diffusion along grain boundaries [16] and reactive diffusion is considered in works [17–19]. The model [17] is applied to explain the growth of silicide between metal and silicon. It

is assumed that the columnar grain boundaries of silicide are perpendicular to the interface between the parent metal and the growing phase, diffusion proceeds predominantly along the grain boundaries, and their collective influence is accounted for through structural parameters that are formally introduced from physical considerations for an individual intergrain boundary. In Ref. [18] it is argued that there is one essential difference between grain boundary diffusion in the presence and in the absence of chemical compound formation, associated with the presence of an equilibrium phase boundary at the growth boundary. In order for the newly formed phase to grow, enough material must arrive at the growth boundary to satisfy the minimum requirements for the composition of the new phase. The two-dimensional model corresponds to two grains of the same size with an intergrain boundary between them, which is located between the original phases. The interfaces are perpendicular to the intergrain boundary. Numerical calculations by the authors show that in physically reasonable situations, there is a linear concentration profile at and around the grain boundary corresponding to stationary conditions. The authors of Ref. [19] analyse the kinetics of reactive diffusion in a hypothetical binary system and assume that a single intermetallic compound can form between the two primary phases. The interface between the phases is assumed to be flat; the reasoning leads the authors to a one-dimensional problem in which the growth rate of a new phase is controlled by the mutual diffusion coefficient.

In the review [20] it is stated that diffusion along grain boundaries accompanied by the formation of new phases can be one of the reasons for the migration of grain boundaries and the formation of new grains. Grain growth in the process of reactive diffusion in Ref. [21] is directly related to the formation of intermetallic compounds. The author proposed two models: (1) solid-phase reaction and grain-boundary diffusion occur simultaneously and (2) transverse grain growth occurs due to diffusion, followed by a sequential chemical reaction. In Refs. [22–24], when modelling the formation of the oxide layer in intermetallides, it is assumed that reactions take place both in the volume and in clearly separated grain boundaries (in the boundary phase). The boundaries separating the oxide phases from the initial phases are not explicitly distinguished in the model, but can be determined using direct calculations from the additional condition. A similar approach to modelling of the surface treatment process with explicit separation of diffusion in the volume and along grain boundaries is used in Ref. [25].

In general, a great number of works are devoted to diffusion and phase formation in binary systems. A part of them refers to real systems, while another part refers to hypothetical systems, thermodynamic justification and modelling issues of fundamental character. Thus, the theory of "mutual consumption" proposed in Ref. [26] and used in Ref. [27] to describe the growth of multilayer films does not explicitly consider the distribution of concentrations in the phases. The theory uses the assumption of the existence of a well-defined stoichiometric composition and structure for each layer and the existence of equilibrium conditions at the phase boundaries. The overall reaction occurring at a particular interphase boundary is determined by the ratio of the rates of accumulation of atoms A and B at this boundary and takes into account that the growth rate of any phase affects the growth and/or absorption of neighbouring phases. Another variant of the theory [28], which takes into account the relationship between reaction rates at each of the boundaries and the number of atoms of the interacting components absorbed in the reaction depending on their stoichiometry, leads to similar equations for the positions of the interfaces. Reactive diffusion in a binary system, due to which layers of chemical compounds (intermetallides, silicides, oxides, etc.) are formed, is analysed in Ref. [29]. The author considers the formation of a new phase as a result of two "different" chemical reactions at the boundaries with the initial phases; he distinguishes critical thicknesses and modes of layer growth. The presence of a critical thickness is associated with a slowdown in the diffusion of reactants through the reaction product layer [30]. The author of Refs. [31,32] analyses the kinetics of reactive diffusion in a hypothetical binary system consisting of one intermetallic compound and two primary phases of solid solutions. The interface migration is assumed to be controlled by bulk diffusion in the neighbouring phases. According to the obtained solution, the square of the intermetallic compound thickness increases proportionally to the annealing time, and the main parameters controlling the growth rate are the diffusion coefficient and the solubility range of the intermetallic compound. For the same hypothetical binary system, the influence of the temperature dependence of the solubility of each phase on the kinetics of reactive diffusion has been analysed. In Ref. [33] the Stefan's condition is explicitly recorded at the interfaces, the drift velocity of the interfaces is introduced, which is related to the Kirkendall effect. The binary system is also analysed in Ref. [8], where the vacancy flux is included in the flux balance, and the equilibrium conditions of the phases are written directly using chemical potentials. In Ref. [34], it is shown that taking into account non-ideal sources and sinks of vacancies we can study not only the thickness of layers of individual phases in time, but also reveal the role of the Kirkendall effect ("change in the distance between markers due to local swelling/compression caused by generation/annihilation of vacancies"), and the

evolution of concentration profiles in individual phases. Non-equilibrium vacancies are also taken into account in earlier works [35]. In Ref. [36], the author specifies some criteria for the growth of phases and points out that a given phase grows the faster the greater the mutual diffusion coefficient in the phase, the wider the homogeneity region of the phase, the closer the phase is to the edge of the diffusion zone, the smaller the initial concentration difference of the initial components of the diffusion pair, and the smaller the diffusion parameters of the other simultaneously growing phases.

Problems based on the theory of reactive diffusion were formulated when analysing the sintering process of powders containing metal shavings as a waste product of metalworking production. Due to the heterogeneous composition of Ti-Al-(Fe+C)-Fe_2O_3 powder pressings, different sequences of diffusion-controlled processes are realised in different parts of the sample under sintering conditions [1,2], which lead to different variants of diffusion-chemical problems with moving boundaries [37–39]. Depending on the temperature range, the sequence of stages can also change.

It is known that when the diffusion rate is much higher than the chemical reaction rate, the process of growth of a new phase is controlled by the chemical reaction. Under such conditions, the time dependence of the thickness of the new phase layer can have an almost linear character. In the opposite situation, if the diffusion process is the controlling factor (the slowest stage), the time dependence of the oxide thickness is usually parabolic. However, in most situations one cannot ignore both diffusion and chemical processes [40 42]. In addition, chemical, diffusion and mechanical processes are closely interrelated, which requires the creation of appropriate models.

2.2. Chemical stresses during reactive diffusion

The interaction products are refractory and have different physical and mechanical properties, which leads to the appearance of chemical stresses in local regions, which can be estimated on the basis of approximate analytical solutions. Both the analysis of possible mechanisms of phase formation within the framework of the reactive diffusion theory and the calculation of mechanical stresses accompanying phase formation processes each time represent a separate problem and require additional assumptions. This entails the appearance of numerous publications with different applications.

Thus, when studying the mutual influence of diffusion and stresses in a hollow cylinder in Ref. [43], an explicit expression for the hydrostatic stress following from the solution of the equilibrium problem taking into account diffusion stresses was used. This allowed the authors to introduce an effective diffusion coefficient related to the elastic modulus and partial molar volume. The authors established a quantitative difference in the concentration profiles for a cylinder with a given constant surface potential and with a constant surface stress. The change in composition associated with the appearance of new phases is not analysed in this work.

When building a model of oxidation of SiC fibres, the authors of Ref. [40] take into account that the oxidant diffuses through the oxide due to chemical potential differences, chemical reactions occur at the interface between the oxide and the substrate, at the interface there is often a significant volume swelling caused by the phase transformation of the starting material into the oxide. Large elastic-viscoplastic deformations can occur. The authors [40] solve the problem of oxide layer growth in the diffusion-kinetic approximation, without distinguishing explicit boundaries, but take into account the change in the diffusion activation energy [44] with hydrodynamic pressure (hydrostatic stress), which follows from the mechanical part of the problem.

The solution of the hollow ball equilibrium problem was used in Ref. [45] to estimate the mechanical stresses in it associated with the different arrangement of aluminium and copper layers, between which intermediate phases could be formed. The change of volume due to the change of composition is attributed by the authors to plastic relaxation, although the defining relations are similar to those used in the theory of thermoelastic diffusion. Near the interfaces, the stresses exceeded 1 GPa. A similar approach to stress estimation was used in Ref. [46] to describe reactive diffusion and associated stresses in a cylindrically shaped nanostructure. The authors emphasise the volume change due to the generation and annihilation of vacancies, and in recording the fluxes of the components they take into account the change in their chemical potentials due to the change in the potential of the vacancies and the hydrostatic pressure defined through the first invariant of the stress tensor. The conditions at the interfaces are not explicitly formulated by the authors in either paper.

About chemical stresses many authors [47–49] speak only because at formulation of the diffusion problem the expression for the chemical potential is used explicitly. Formation of new phases does not occur at that. In particular, Ref. [47] analyses the stresses induced by radial diffusion into an incompressible solid sphere, which is considered isotropic and elastic. Linear and nonlinear theory options are considered. In Ref. [48] the important role of anisotropy in modelling diffusion-induced stresses is emphasised. The model discussed in Ref. [49] formally takes into account the dependence of the Li-Si reaction rate on the crystallographic orientation and plasticity at large strains: a sharp phase boundary with a sharp change in Li

concentration is a consequence of the concentration dependence of the diffusion coefficient. The chemical transformations proper are not modelled. In Ref. [50], the solutions of coupled (taking into account the influence of stresses on diffusion) and uncoupled problems (without taking stresses into account) for a spherical cell of a lithium-ion battery without a change in the phase state are compared. In Ref. [51] it was shown that the contribution of diffusion-induced stresses to the overall stress state of the crystal during growth can be comparable to the contribution from thermal stresses. In Ref. [52], a relationship between surface energy, surface tension and the magnitude of diffusion-induced stresses in nanowires was postulated. The authors showed that diffusion induced stresses, especially tensile stresses, can be significantly reduced by surface effects. In Ref. [53], it is shown that changing the elastic modulus with composition can slow down or accelerate the redistribution of concentrations. The authors of Ref. [54] indicate that chemical stresses are associated with diffusion accelerated mass transfer. In their opinion, the condition of constant chemical potential at the boundary is more consistent with real conditions than concentration constancy.

There are generalised theories, the analysis of which requires special consideration. Let us note only some of them. Thus, the density tensor, tensors of concentration of components, tensors of chemical potentials and mass fluxes as tensors of the third rank are introduced in Ref. [55] at construction of the diffusion theory for metals. In this case the diffusive flux of matter is associated not only with the gradient of the volume expansion (or the trace of the stress tensor), but also induced by the gradients of each of the components of the strain (or stress) tensor. A series of papers by F.C. Larche and J.W. Cahn [56–58] is devoted to the analysis of general relations for chemical potentials and the establishment of conditions at interfaces. The authors showed that different equilibrium conditions are obtained depending on the presence or absence of vacancies and on which of the three types of contact takes place—coherent or incoherent interfaces, solid-solid or solid-liquid interfaces. The authors point out that in some particular cases of geometries the influence of stresses on diffusion is reduced to an additional dependence of the diffusion coefficient on concentrations, but this is not the only factor that should be taken into account. Problems of construction of generalised theories of matter transport in solids, including nonlocality and memory effects, are discussed in Ref. [59]. The author emphasises that it is the introduction of suitable defining relations that allows one to distinguish, for example, diffusion in stressed and unstressed solids, diffusion of viscous and non-viscous solution or diffusion in elastic and inelastic materials. The paper presents a formula for diffusion in a nonlinear stress field and gives a brief discussion of diffusion in a nonlinear elastic body. The theories of Fick and Darcy types are obtained as special cases of this model.

V.S. Eremeev [60] gives a generalisation of the theory of diffusion by replacement and introduction of mechanisms for an elastic isotropic body and for a viscoelastic isotropic body of general form. At the same time, he gives solutions of equilibrium problems for bodies of the simplest geometrical forms (plate, cylinder, sphere), which are actually repeated with different variations in numerous publications of the last years [61,62]. The authors of Refs. [63,64], when constructing a model of a solid medium with diffusion, use a multiplicative representation of the strain rate tensor and distinguish eigenstrains due to composition changes and viscous deformations at high temperatures. And in Refs. [65,66] the theory of chemical diffusion under the action of electromagnetic field is proposed. As a result, linear defining relations in the same form as in classical linearised models of thermoelastic diffusion are obtained. The authors claim that they have developed a thermodynamically consistent continuum theory of coupled deformation, mass diffusion, heat conduction and chemical reactions. However, the degree of transformation or reaction coordinate has long been used in the thermodynamic description of chemically reacting systems simultaneously with the concentrations of the components [67–69].

Gradient mechanisms of elastic deformation are taken into account in Refs. [70,71] when building models of media with diffusion and chemical reactions. The authors claim that such approaches are useful in constructing models of physicochemical processes for nano- and microscale structures. In Ref. [72], a micropolar approach is used to derive the defining relations and then the inhomogeneous stress-strain state of a cylindrical metallic sample is modelled. The boundary condition used in the considered boundary value problem reflects the influence of structural defects located at the boundary. The diffusion coefficient depends on the temperature according to the Arrhenius law, with the diffusion activation energy depending on the strain energy. It is also emphasised in Ref. [73] that stresses can also influence the diffusion process through additional terms in the diffusion equation, as well as through a change in the diffusion activation energy through a change in chemical affinity [74,75]. The authors consider the latter effect to be determinant.

In the present work we consider solutions of partial problems of the reaction diffusion theory, which model the processes of phase formation during sintering in the complex system Ti-Al-Fe-Fe_2O_3 with the use of quasi-stationary approach. At the same time, we estimate local stresses associated with the appearance of new phases on the basis of the traditional approach.

3. PHASE FORMATION IN THE Ti-Al-Fe-Fe_2O_3 SYSTEM

3.1. Particular problems of the theory of reaction diffusion with reducing stages

So, from the chemical point of view, reactive diffusion is a solid-phase reaction controlled by the supply of reactants through the layers of reaction products. From the physical point of view, reactive diffusion is a chain of competitive phase transformations in the concentration gradient in the diffusion zone [76]. If in a system of two metals (diffusion proceeds by the mechanism of substitution) or in a metal-gas system (diffusion proceeds by the mechanism of introduction) with the formulation of problems and the choice of diffusion coefficients all is more or less clear, then in a complex system in which there can occur both the reaction of substitution of one metal by another in an oxide and sequential or parallel reactions of intermetallide formation, the problems on phase formation become very tentative. However, even in this case they are undoubtedly useful. For the solution of all diffusion-kinetic problems we use the quasi-stationary approach, so we will show in detail the solution only on some examples.

3.1.1. Al-Fe_2O_3 system

According to Refs. [9–14], the following reactions are possible in Al-Fe_2O_3 system:

$2Al + Fe_2O_3 = Al_2O_3 + 2Fe$,

$2Fe_2O_3 \rightarrow 4FeO + O_2$,

$FeO + Al_2O_3 = FeAl_2O_4$,

$9Fe_2O_3 + 2Al = 6Fe_3O_4 + Al_2O_3$,

$3Fe + Al = Fe_3Al$.

The presence of $FeAl_2O_4$ double oxide and Fe_3Al phase in the products depends on the ratio of Fe_2O_3 and Al powders in the initial mixture and the presence of oxide film on aluminium. We consider that reprecipitation starts at the melting temperature of aluminium. The melt surrounds the iron oxide particle from all sides. The size of the areas occupied by the initial phases (R_p and R_m) depends on the ratio of components in the initial mixture.

Limiting ourselves to two total phases, resulting in the formation of aluminium oxide and a mixture of intermetallides with the total composition Fe_xAl_y, and assuming that the refractory iron oxide particle (compared to aluminium) has a spherical shape, the sequence of phases will be depicted as shown in Fig. 3.

We assume that the size of the total oxide particle R_p, which includes Fe_2O_3 and Al_2O_3 oxides, does not change, so that in our problem there will be only two moving

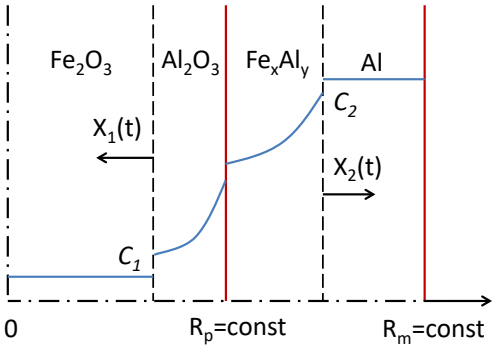

Fig 3. The sequence of phases in the Fe_2O_3-Al system (without taking into account the formation of solution and double oxide).

boundaries, between the oxides X_1 and between the intermetallide and aluminium X_2. As a result, the reaction diffusion problem will take the following form:

$$\frac{\partial C_k}{\partial t} = \frac{1}{r^2}\frac{\partial}{\partial r}\left(r^2 D_k \frac{\partial C_k}{\partial r}\right); \tag{7}$$

$$r = 0: \ \frac{\partial C_{Fe_2O_3}}{\partial r} = 0; \tag{8}$$

$$r = X_1(t): \ C_{Fe_2O_3} = C_0, \ C_{Al_2O_3} = C_1, \tag{9}$$

$$\left(C_{Fe_2O_3} - C_{Al_2O_3}\right)\frac{dX_1}{dt} = -D_{Fe_2O_3}\frac{\partial C_{Fe_2O_3}}{\partial r} + D_{Al_2O_3}\frac{\partial C_{Al_2O_3}}{\partial r}; \tag{10}$$

$$r = R_p = \text{const}: \ C_{Al_2O_3} = \gamma C_{Fe_xAl_y};$$

$$D_{Al_2O_3}\frac{\partial C_{Al_2O_3}}{\partial r} = D_{Fe_xAl_y}\frac{\partial C_{Fe_xAl_y}}{\partial r}; \tag{11}$$

$$r = X_2(t): \ C_{Fe_xAl_y} = C_2, \ C_{Al} = 1, \tag{12}$$

$$\left(C_{Fe_xAl_y} - C_{Al}\right)\frac{dX_2}{dt} = -D_{Fe_xAl_y}\frac{\partial C_{Fe_xAl_y}}{\partial r} + D_{Al}\frac{\partial C_{Al}}{\partial r}; \tag{13}$$

$$r = R_m: \ \frac{\partial C_{Al}}{\partial r} = 0.$$

Here index k = Fe_2O_3, Al_2O_3, Fe_xAl_y, Al corresponds to the area occupied by the phase; C_k is the concentration of alumina in these phases. Condition (8) is a symmetry condition; (9), (10) and (12), (13) are conditions on mobile boundaries separating new and old phases; condition (11) corresponds to an ideal contact between phases, but includes different mobility of diffusant in phases; the last condition is a condition of absence of sources and sinks on the matrix (aluminium) boundary, falling on one particle. The size of the calculated area is calculated by the formula:

$$R_m = \frac{R_p}{\sqrt[3]{\eta_0}},$$

where η_0 is given initial volume fraction of particles. At the initial moment of time there is only aluminium and iron oxide.

In the quasistationary approximation instead of Eq. (7) we have stationary equations:

$$\frac{1}{r^2}\frac{d}{dr}\left(r^2 D_k \frac{dC_k}{dr}\right)=0.$$

In the area of aluminium $C_{\mathrm{Al}}=1$; in the area of iron oxide $C_{\mathrm{Al}}=C_0=0$. In the new phases, the concentration distributions have the form:

$$C_k(r)=-\frac{A_k}{r}+B_k. \tag{14}$$

where $k=1$ and $k=\mathrm{Al_2O_3}$ denote oxide area $\mathrm{Al_2O_3}$, $k=2$ and $k=\mathrm{Fe}_x\mathrm{Al}_y$ denote intermetallide area.

From conditions (9), (11) and (12) we find a system of linear equations for determining the integration constants:

$$-\frac{A_1}{X_1}+B_1=C_1,$$
$$-\frac{A_2}{X_2}+B_2=C_2,$$
$$-\frac{A_1}{R_p}+B_1=\gamma\left(-\frac{A_2}{R_p}+B_2\right),$$
$$D_{\mathrm{Al_2O_3}}\frac{A_1}{R_p^2}=D_{\mathrm{Fe}_x\mathrm{Al}_y}\frac{A_2}{R_p^2}.$$

The solution of this system has the form:

$$A_1=\frac{D_{\mathrm{Fe}_x\mathrm{Al}_y}\left(X_1X_2R_p\right)\left(\gamma C_2-C_1\right)}{D_{\mathrm{Fe}_x\mathrm{Al}_y}X_2\left(R_p-X_1\right)-\gamma D_{\mathrm{Al_2O_3}}X_1\left(R_p-X_2\right)},$$

$$A_2=\frac{D_{\mathrm{Al_2O_3}}\left(X_1X_2R_p\right)\left(\gamma C_2-C_1\right)}{D_{\mathrm{Fe}_x\mathrm{Al}_y}X_2\left(R_p-X_1\right)-\gamma D_{\mathrm{Al_2O_3}}X_1\left(R_p-X_2\right)},$$

$$B_1=C_1+\frac{A_1}{X_1},\quad B_2=C_2+\frac{A_2}{X_2}.$$

Since the positions of the interfaces change in time, the integration constants also depend on time.

Using the obtained solution, from conditions (10) and (13) we find the equations for determining the position of the phase boundaries:

$$-C_1\frac{dX_1}{dt}=\frac{X_2R_p}{X_1}\frac{D_{\mathrm{Al_2O_3}}D_{\mathrm{Fe}_x\mathrm{Al}_y}\left(\gamma C_2-C_1\right)}{D_{\mathrm{Fe}_x\mathrm{Al}_y}X_2\left(R_p-X_1\right)-\gamma D_{\mathrm{Al_2O_3}}X_1\left(R_p-X_2\right)},$$

$$\left(C_2-1\right)\frac{dX_2}{dt}=$$
$$-\frac{X_1R_p}{X_2}\frac{D_{\mathrm{Fe}_x\mathrm{Al}_y}D_{\mathrm{Al_2O_3}}\left(\gamma C_2-C_1\right)}{D_{\mathrm{Fe}_x\mathrm{Al}_y}X_2\left(R_p-X_1\right)-\gamma D_{\mathrm{Al_2O_3}}X_1\left(R_p-X_2\right)}. \tag{15}$$

It is convenient to solve the system of ordinary differential equations by the Euler method, assuming that at the initial moment of time the boundaries are separated from R_p by some small distance.

Knowing the position of the interface, we can determine the size of the areas occupied by the phases and calculate their volume fractions:

$$\eta_{\mathrm{Fe_2O_3}}=X_1^3/R_m^3,\quad \eta_{\mathrm{Al_2O_3}}=\left(R_p^3-X_1^3\right)/R_m^3,$$
$$\eta_{\mathrm{Fe}_x\mathrm{Al}_y}=\left(X_2^3-R_p^3\right)/R_m^3,\quad \eta_{\mathrm{Al}}=\left(R_m^3-X_2^3\right)/R_m^3.$$

In calculations the Arrhenius dependence of diffusion coefficient on temperature is assumed:

$$D_{ph,i}=D_{0,i}\exp\left(-\frac{E_i}{RT}\right),$$

and the temperature is set to $T=1100$ K.

The concentration distribution and the position of the boundaries for this problem are given in Fig. 4 for different moments of time. Data for diffusion coefficients are given in Table 1.

Since the metal chips used in the experiments [37–39] are rather flat objects, considering such a problem in the Cartesian coordinate system, we obtain linear distributions of concentrations

$$C_k(x)=A_kx+B_k, \tag{16}$$

where

$$A_1=\frac{D_{\mathrm{Fe}_x\mathrm{Al}_y}\left(\gamma C_2-C_1\right)}{D_{\mathrm{Fe}_x\mathrm{Al}_y}\left(R_p-X_1\right)-\gamma D_{\mathrm{Al_2O_3}}\left(R_p-X_2\right)},$$
$$A_2=\frac{D_{\mathrm{Al_2O_3}}\left(\gamma C_2-C_1\right)}{D_{\mathrm{Fe}_x\mathrm{Al}_y}\left(R_p-X_1\right)-\gamma D_{\mathrm{Al_2O_3}}\left(R_p-X_2\right)},$$
$$B_1=C_1-A_1X_1,\quad B_2=C_2-A_2X_2,$$

and equations for moving boundaries of the form

$$-C_1\frac{dX_1}{dt}=\frac{D_{\mathrm{Fe}_x\mathrm{Al}_y}D_{\mathrm{Al_2O_3}}\left(\gamma C_2-C_1\right)}{D_{\mathrm{Fe}_x\mathrm{Al}_y}\left(R_p-X_1\right)-\gamma D_{\mathrm{Al_2O_3}}\left(R_p-X_2\right)},$$

$$\left(C_2-1\right)\frac{dX_2}{dt}=-\frac{D_{\mathrm{Fe}_x\mathrm{Al}_y}D_{\mathrm{Al_2O_3}}\left(\gamma C_2-C_1\right)}{D_{\mathrm{Fe}_x\mathrm{Al}_y}\left(R_p-X_1\right)-\gamma D_{\mathrm{Al_2O_3}}\left(R_p-X_2\right)}. \tag{17}$$

Table 1. Data used to calculate diffusion coefficients for phase formation in the system Fe_2O_3-Al [77].

Phase	D_0, m²/s	E, kJ/mol
Al_2O_3	$5\cdot10^4$	380
Fe_xAl_y	$1.46\cdot10^{-3}$	223
$FeAl_2O_4$	$4.6\cdot10^{-7}$	162
Fe(Al)	$1.46\cdot10^{-3}$	223

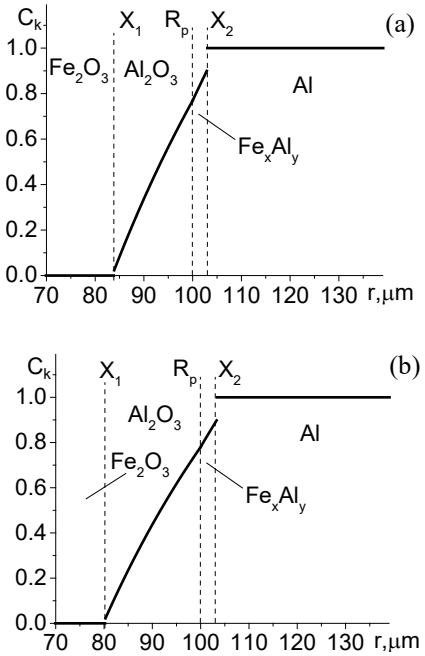

Fig. 4. Distribution of aluminium concentration in the formed new phases at different moments of time: (a) $t = 70$ s; (b) $t = 100$ s. $C_1 = 0.02$, $C_2 = 0.9$, $\gamma = 1$, $R_p = 100$ μm, $\eta_0 = 0.2$, $T = 1100$ K.

It follows from Eq. (15) that

$$X_1^3 = -X_2^3 + R_p^3\left(1+\frac{C_1}{1-C_2}\right),$$

and from Eq. (17) that

$$X_1 = -X_2 + R_p\left(1+\frac{C_1}{1-C_2}\right).$$

A comparison of the interface dynamics for the planar and spherical problems is given in Fig. 5. For the boundary separating intermetallide from aluminium, we obtain very close laws, while the boundary separating oxides changes differently. By a certain moment of time the substitution reaction in the spherical particle is completed, while in the case of the planar particle there is a slowing down of the growth of the Al_2O_3 phase. The interfaces in each case move according to the same laws, but the rates of phase formation are different and depend on the value of the $C_1/(1-C_2)$.

This cannot be said when taking into account the possible formation of other phases in the system. For example, assuming that the formation of an intermetallide on the aluminium side is preceded by the formation of a solid solution, we arrive at a problem corresponding to Fig. 6a.

For variant in Fig. 6a, the problem for the Cartesian coordinate system is solved in the approximation of the constructed size of the total oxide particle. The conditions

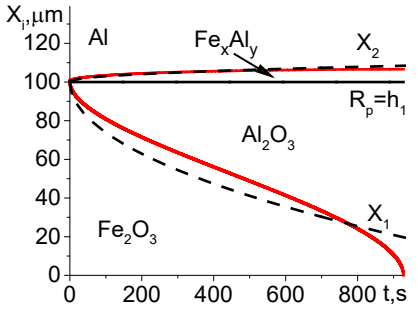

Fig. 5. Interface dynamics during the formation of two new phases in the Fe_2O_3-Al system. Solid and dashed lines correspond to the solutions in the spherical and Cartesian (for a flat particle) coordinate systems, respectively.

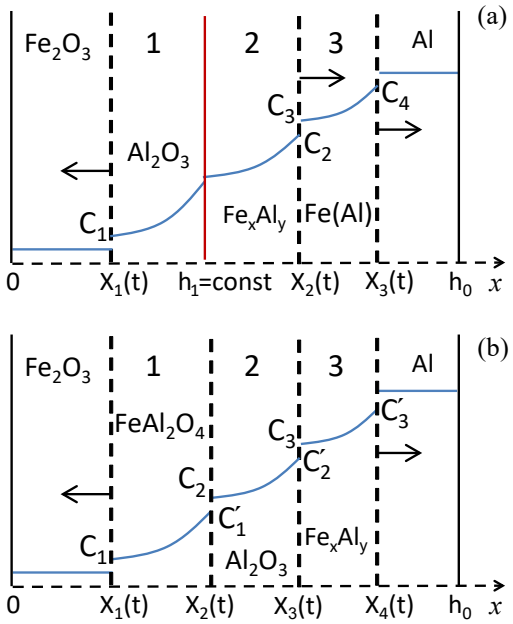

Fig. 6. Sequence of three phases in the Fe_2O_3–Al system (a) with solution formation; (b) with double oxide formation.

at the fixed boundary and at the mobile interfaces are formulated similarly to the previous one. The concentration distributions in the phases have the form (16), where the six integration constants are found explicitly from the six boundary conditions and have the following form:

$$A_1 = \frac{(\gamma C_2 - C_1)}{(h_1 - X_1) - \gamma\theta(h_1 - X_2)},\ A_2 = \theta A_1,\ A_3 = \frac{(C_4 - C_3)}{X_3 - X_2},$$

$$B_1 = C_1 - A_1 X_1,\ B_2 = C_2 - A_2 X_2,\ B_3 = C_4 - A_3 X_3, \qquad (18)$$

where

$$\theta = \theta(T) = \frac{D_{Al_2O_3}}{D_{Fe_xAl_y}}.$$

The equations for the interfaces are fully coupled and analytical estimates are not possible:

$$C_1\frac{dX_1}{dt}=-\frac{D_{Al_2O_3}\left(\gamma C_2-C_1\right)}{\left(h_1-X_1\right)-\gamma\theta\left(h_1-X_2\right)},$$

$$\left(C_2-C_3\right)\frac{dX_2}{dt}=$$
$$-\frac{D_{Al_2O_3}\left(\gamma C_2-C_1\right)}{\left(h_1-X_1\right)-\gamma\theta\left(h_1-X_2\right)}+D_{Fe(Al)}\frac{\left(C_4-C_3\right)}{X_3-X_2},$$

$$\left(C_4-1\right)\frac{dX_3}{dt}=-D_{Fe(Al)}\frac{\left(C_4-C_3\right)}{X_3-X_2}. \qquad (19)$$

This system was solved numerically using Euler's method.

The interface dynamics is shown in Fig. 7a. The aluminium oxide phase grows the fastest at the chosen set of parameters (Table 1). This is also shown in Fig. 7b, which shows the change of volume fractions of phases in time. The distributions of alumina concentration in the phases by the time 400 s are shown in Fig. 7c. It is accepted according to equilibrium state diagrams [78,79]: $C_1=0.01$, $C_2=0.72$, $C_3=0.73$, $C_4=0.98$.

In the spherical coordinate system, we have distributions (14) in each of the three phases:

$$C_{Al_2O_3}\left(r\right)=-\frac{A_1}{r}+B_1,$$

$$C_{Fe_xAl_y}\left(r\right)=-\frac{A_2}{r}+B_2,$$

$$C_{Fe(Al)}\left(r\right)=-\frac{A_3}{r}+B_3.$$

In this case, to find the integration constants we have a system of six linear equations

$$r=X_1\left(t\right):\ -\frac{A_1}{X_1}+B_1=C_1;$$

$$r=R_p:\ -\frac{A_1}{R_p}+B_1=\gamma\left(-\frac{A_2}{R_p}+B_2\right),$$
$$D_{Al_2O_3}\frac{A_1}{R_p^2}=D_{Fe_xAl_y}\frac{A_2}{R_p^2};$$

$$r=X_2\left(t\right):\ -\frac{A_2}{X_2}+B_2=C_2,\ -\frac{A_3}{X_2}+B_3=C_3;$$

$$r=X_3\left(t\right):\ -\frac{A_3}{X_3}+B_3=C_4,$$

the solution of which is conveniently represented in the form:

$$A_1=\frac{X_1X_2R_p\left(\gamma C_2-C_1\right)}{X_2\left(R_p-X_1\right)-\gamma\theta X_1\left(R_p-X_2\right)},\quad A_2=\theta A_1,$$

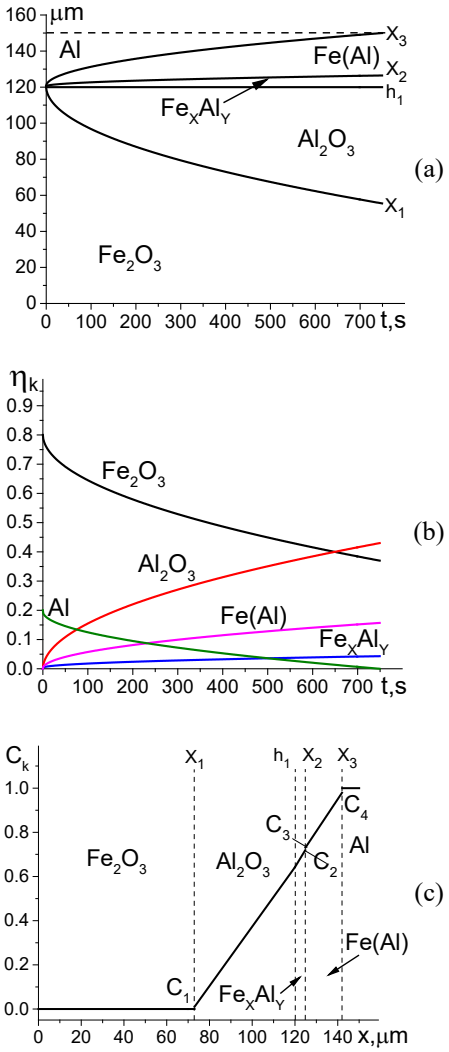

Fig. 7. Dynamics of interface (a), volume fractions of phases (b) and concentration distribution (c) at the time t = 400 s. Calculation was carried out at T = 1100 K.

$$B_1=C_1+\frac{A_1}{X_1},\quad B_2=C_2+\frac{A_2}{X_2},$$

$$A_3=\frac{\left(C_4-C_3\right)X_3X_2}{X_3-X_2},\quad B_3=\frac{C_4X_3-C_3X_2}{X_3-X_2}. \qquad (20)$$

The equations for the three moving interfaces are obtained from the conditions for flows similar to Eqs. (10) and (13):

$$-C_1\frac{dX_1}{dt}=D_{Al_2O_3}\frac{A_1}{X_1^2},$$

$$\left(C_2-C_3\right)\frac{dX_2}{dt}=\left[-D_{Fe_xAl_y}\frac{A_2}{X_2^2}+D_{Fe(Al)}\frac{A_3}{X_2^2}\right],$$

$$\left(C_4-1\right)\frac{dX_3}{dt}=-D_{Fe(Al)}\frac{A_3}{X_3^2}. \qquad (21)$$

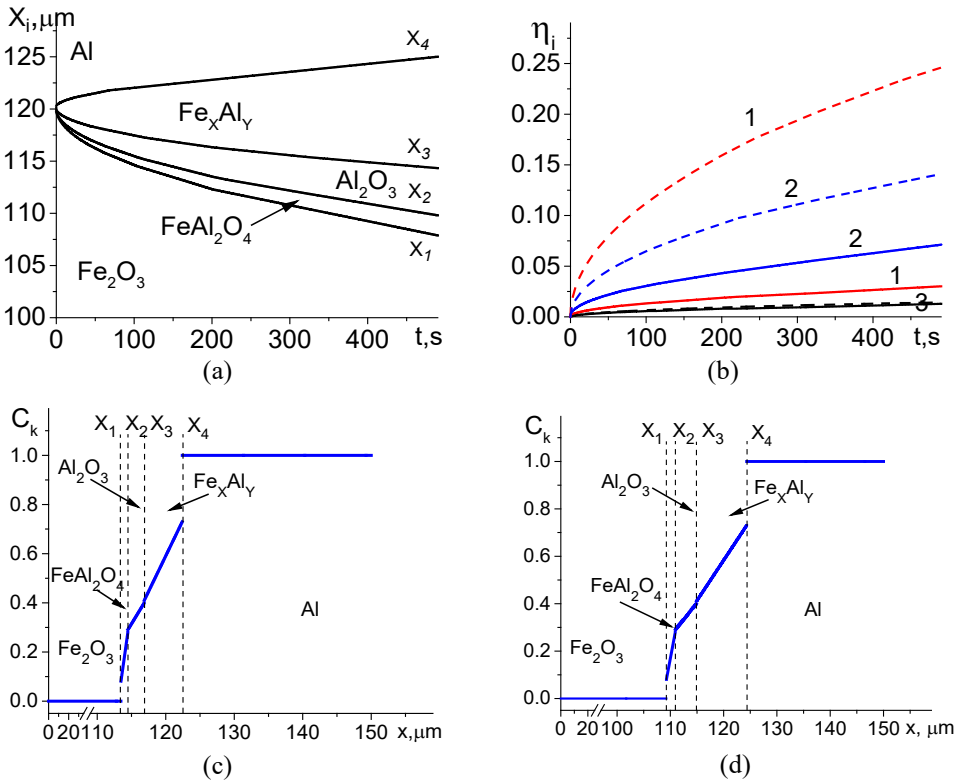

Fig. 8. Dynamics of interface boundaries (a), volume fractions of phases (b) and diffusant concentration distribution in phases at different time moments: t = 100 s (c) and t = 400 s (d) during phase formation in Fe_2O_3-Al system taking into account the possible appearance of double oxide. Parameter values: T = 1100 K; $C_1 = 0.08$, $C_1' = 0.28$, $C_2 = 0.29$, $C_2' = 0.4$, $C_3 = 0.41$, $C_3' = 0.73$. In subfigure (b): 1 – Al_2O_3; 2 – Fe_xAl_y; 3 – $FeAl_2O_4$; solid lines – T = 1100 K; dashed lines – T = 1200 K.

For the situation shown in Fig. 6b, we come to the problem with four moving interfaces. But the number of new phases is still three. In this case, in the distribution (16) for the Cartesian coordinate system, taking into account the notations in Fig. 6b, we come to the problem with four moving phase boundaries:

$$A_1 = \frac{(C_1' - C_1)}{X_2 - X_1}, \quad B_1 = \frac{C_1 X_2 - C_1' X_1}{X_2 - X_1},$$
$$A_2 = \frac{(C_2' - C_2)}{X_3 - X_2}, \quad B_2 = \frac{C_2 X_3 - C_2' X_2}{X_3 - X_2},$$
$$A_3 = \frac{(C_3' - C_3)}{X_4 - X_3}, \quad B_3 = \frac{C_3 X_4 - C_3' X_3}{X_4 - X_3}, \qquad (22)$$

and

$$C_1 \frac{dX_1}{dt} = -D_1 \frac{(C_1' - C_1)}{X_2 - X_1},$$

$$(C_1' - C_2)\frac{dX_2}{dt} = \left[-D_1 \frac{(C_1' - C_1)}{X_2 - X_1} + D_2 \frac{(C_2' - C_2)}{X_3 - X_2} \right],$$

$$(C_2' - C_3)\frac{dX_3}{dt} = \left[-D_2 \frac{(C_2' - C_2)}{X_3 - X_2} + D_3 \frac{(C_3' - C_3)}{X_4 - X_3} \right],$$

$$(C_3' - 1)\frac{dX_4}{dt} = -D_3 \frac{(C_3' - C_3)}{X_4 - X_3}. \qquad (23)$$

where $D_1 = D_{FeAl_2O_4}$, $D_2 = D_{Al_2O_3}$, $D_3 = D_{Fe_xAl_y}$ are aluminium diffusion coefficients in phases. As above, we can calculate the volume fractions of phases:

$$\eta_{Fe_2O_3} = X_1/h_0, \quad \eta_{FeAl_2O_4} = (X_2 - X_1)/h_0,$$
$$\eta_{Al_2O_3} = (X_3 - X_2)/h_0, \quad \eta_{Fe_xAl_y} = (X_4 - X_3)/h_0,$$
$$\eta_{Al} = (h_0 - X_4)/h_0.$$

The results of calculations are presented in Fig. 8. The aluminium oxide phase is located between the boundaries X_2 and X_3. In this case, its share in the total volume of phases grows slower than in the previous case. The fastest growth is observed for the intermetallic phase. Note that the rules derived in Ref. [36] for the fastest growing phase can hardly be applied here, since in the real situation there are many kinetic difficulties, such as the existence of oxide films on metals.

3.1.2. Ti-Fe_2O_3 system

The Ti+Fe_2O_3 system seems to be similar to the Al+Fe_2O_3 system. According to the phase diagrams [80–82], several

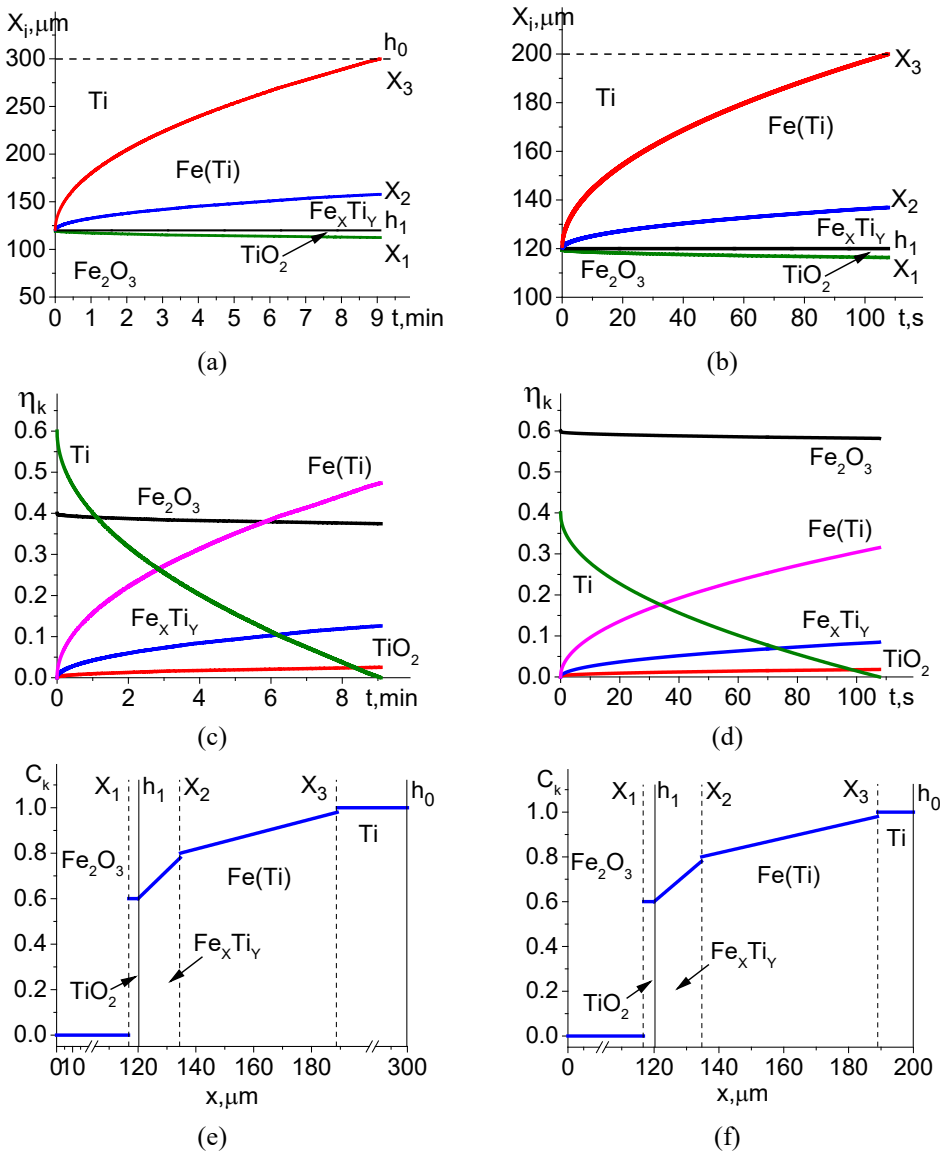

Fig. 9. Dynamics of interfaces (a,b), volume fractions of phases (c,d) and distribution of titanium concentration in phases by the time t = 80 s (e,f) for different initial compositions of the Fe_2O_3-Ti system: on the left – iron oxide volume fraction is 0.4; on the right – 0.6.

ternary phases are possible in the Ti-Fe-O system: Fe_2Ti, FeTiO, $FeTiO_3$, Fe_2TiO_4, Fe_2TiO_5, and in the Ti-Fe system there are two stable compounds: FeTi and $TiFe_2$. Literature data indicate that the Ti_2Fe phase is a metastable compound and can only be obtained by vapour quenching [83] or mechanical alloying methods [84]. Other researchers have reported Ti_2Fe as an oxygen stabilised alloy due to the fact that this phase was obtained by the interaction of Ti and TiFe only in a solid phase reaction, which was observed as the nucleation and growth of a fine Ti/TiFe eutectic with the presence of residual oxygen during synthesis. According to Ref. [85], the following main reactions take place in the Ti-Fe_2O_3 system. The first one is reduction of Fe_2O_3 by titanium to form Fe and TiO_2 oxide:

$$2Fe_2O_3(III) + 3Ti \rightarrow 4Fe + 3TiO_2$$

The system with excess Ti can provide temperatures up to 1800 K, which are higher than the eutectic temperature (~1600 K) in the Fe-Ti system. Therefore, the second stage under conditions of rapid temperature change will be the formation of intermetallic phase Ti_2Fe, which the authors of the article represent as follows:

$$\text{Ti (excess)} + x\text{Fe} \rightarrow \text{Ti (excess)} + y\text{Ti}_2\text{Fe}$$

The problem of reaction diffusion for this system for conditions of solid-phase sintering in the first approximation is similar to the problem for Al+Fe_2O_3 taking into account solution formation. Then in Fig. 6, phase 1 is TiO_2, phase 2 is Fe_xTi_y, and phase 3 is Fe(Ti) solution. The solution is completely similar to the previous one and is not presented here.

For different initial compositions the dynamics of the process is shown in Fig. 9. The following parameters were used in calculations: $h_1 = 120$ μm, $C_1 = 0.6$, $C_2 = 0.78$, $C_3 = 0.8$,

$C_4 = 0.98$. $\gamma = 1$, the diffusion coefficient of titanium was taken as $D_{TiO_2} = 7.7 \cdot 10^{-9}$ m^2/s, $D_{Fe_xTi_y} = 85 \cdot 10^{-14}$ m^2/s, $D_{Fe(Ti)} = 2.6 \cdot 10^{-12}$ m^2/s.

To conclude the section, we present a model of interaction in the Ti-Al-Fe_2O_3 system [39], assuming that the chip can be considered as a flat object, the oxidised part of which is in contact with aluminium. In this case, a reduction reaction takes place. The released iron goes to form intermetallides of the Al-Fe system. Titanium can also interact with the oxide, but due to its high affinity for aluminium, it is most likely that it will pull away aluminium to form intermetallides of another group Ti-Al. In this case, the conditional reaction cell will take the form shown in Fig. 10. We assume that the total size of the region with Al_2O_3 and Fe_2O_3 oxides (shaded in the figure) does not change and is equal to δ. The initial composition of the reactive cell is characterised by three regions: from $-h_2$ to 0 is Ti; from 0 to $h_1 - \delta$ is Al and from $h_1 - \delta$ to δ is Fe_2O_3. Aluminium can move through six regions. In the same figure, the region containing iron and carbon is highlighted. In the first approximation we do not take into account the diffusion of carbon. However, this region participates in the overall balance of phases in the system.

At the outer boundaries of the region we have the conditions:

$$x = -h_2: \ \frac{\partial C_6}{\partial x} = 0 \ \text{ and } \ x = h_1: \ \frac{\partial C_4}{\partial x} = 0.$$

The conditions at the moving boundaries are similar to the previous one, and at the boundary $h_1 - \delta$ there is a perfect contact. At the initial time, the boundaries X_1 and X_3 are close to $h_1 - \delta$; and the boundaries X_2 and X_4 are close to zero. The detailed solution is presented in Ref. [39]. Let us write out here only the final result:

$$\begin{aligned}
&\left(X_1(t) - (h_1 - \delta)\right)^2 = -2\beta t,\\
&X_3 = -\alpha X_1 + (h_1 - \delta)(1 + \alpha),\\
&X_4(t) = -\sqrt{D_5 \frac{C_{51} - C_{50}}{C_{60} - C_{51}} \frac{2}{1+\mu} t},\\
&X_2 = -\mu X_4 = \mu \sqrt{D_5 \frac{C_{51} - C_{50}}{C_{60} - C_{51}} \frac{2}{1+\mu} t},
\end{aligned} \qquad (24)$$

where

$$\alpha = \frac{C_{10} - C_{20}}{C_{30} - C_{40}}, \ \beta = \frac{D_3}{\frac{D_3}{D_2} + \gamma\alpha} \frac{(\gamma C_{30} - C_{20})}{(C_{10} - C_{20})} < 0,$$

$$\mu = \frac{C_{60} - C_{51}}{C_{50} - C_{10}}.$$

Knowing the initial composition of the powder press and using the obtained analytical solution (24), we can determine the composition of the products by the end of the sintering process. At the initial moment of time the volume fractions of phases in the system Ti+Al+Fe_2O_3+(Fe+C) correspond to the ratios of lengths of segments h_2, $h_1 - \delta$, δ and $h_0 - h_1$, i.e.:

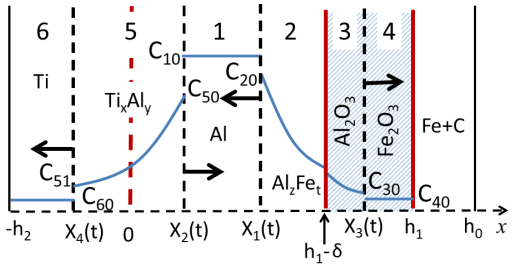

Fig. 10. Sequential arrangement of phases during phase formation in the Ti-Al-Fe_2O_3 system.

$$\eta_{0,Ti} = \frac{h_2}{h_2 + h_0}, \ \eta_{0,Al} = \frac{h_1 - \delta}{h_2 + h_0}, \ \eta_{0,Fe_2O_3} = \frac{\delta}{h_2 + h_0},$$

$$\eta_{0,(Fe+C)} = \frac{h_0 - h_1}{h_2 + h_0}.$$

Here δ is the thickness of oxide film; $h_0 - (h_1 - \delta)$ is chip thickness.

Over time, other phases emerge, with their fractions given as

$$\eta_{Ti} = \frac{X_4 - h_2}{h_2 + h_0}, \ \eta_{Al} = \frac{X_1 - X_2}{h_2 + h_0}, \ \eta_{Fe_2O_3} = \frac{h_1 - X_3}{h_2 + h_0},$$

$$\eta_{Al_2O_3} = \frac{X_3 - (h_1 - \delta)}{h_2 + h_0}, \ \eta_{Ti_xAl_y} = \frac{X_2 - X_4}{h_2 + h_0},$$

$$\eta_{Al_zFe_t} = \frac{h_1 - \delta - X_1}{h_2 + h_0}.$$

The $\eta_{(Fe+C)}$ fraction does not change in this approximation.

Fig. 11 shows a comparison in the dynamics of composition change and in the dynamics of interface for different initial compositions presented in Table 2. Composition 1 corresponds to the dimensions in Fig. 10: $h_1 = 121$ μm, $h_2 = 374$ μm; composition 2 dimensions are $h_1 = 220$ μm, $h_2 = 275$ μm. Diffusion coefficients in phases are the same as above. In calculations it is accepted: $C_{10} = 1$, $C_{20} = 0.72$, $C_{30} = 0.1$, $C_{40} = 0$, $C_{50} = 0.65$, $C_{51} = 0.13$, $C_{60} = 0$. We see that the proposed model responds quite adequately to the change of parameters. At temperature decrease, obviously, diffusion coefficients decrease, which leads to slowing down of phase growth (not shown in the figures).

3.2. Mechanical stresses in localised volumes

To estimate mechanical stresses in the local regions of interaction between the mixture components, we use the same approach as the authors of Refs. [40,43,45,46–50,52–54]. Since the interaction products are refractory,

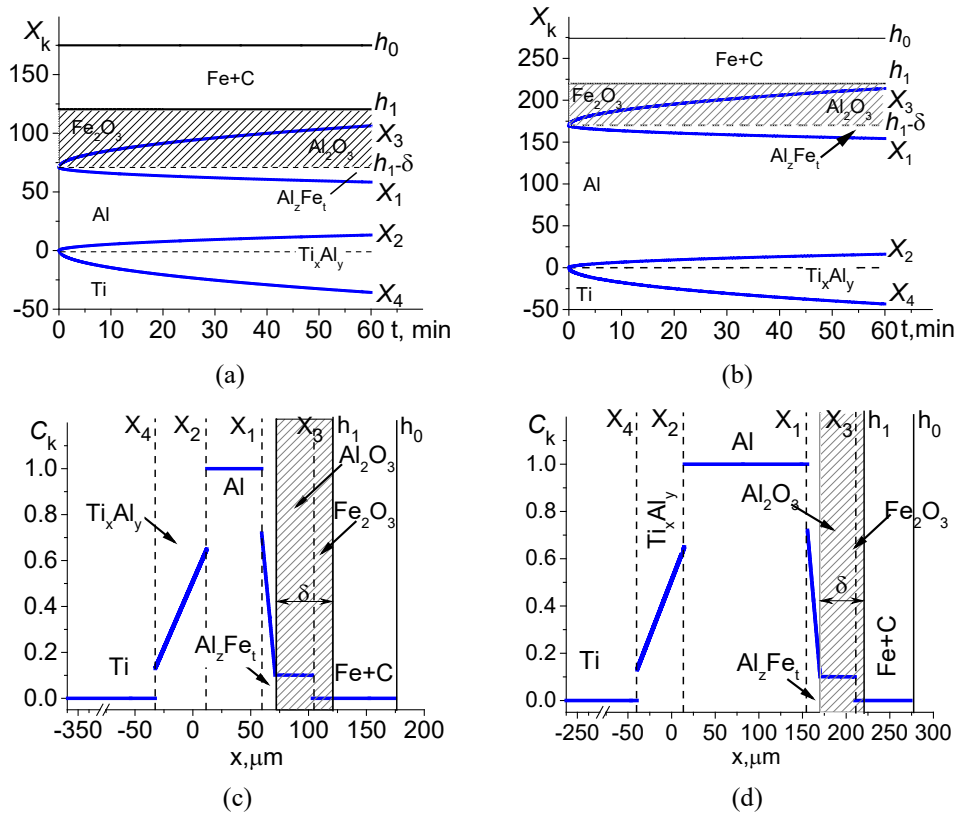

Fig. 11. Position of the interfaces (a,b) and diffusant concentration distribution (c,d) at the time t = 50 min for different initial compositions (Table 2). δ = 50 μm, T = 1300 K, γ = 1.1.

Table 2. Compositions at the initial moment of time and at the end of the process (10% of the total composition is Fe+C).

Phase	Initial composition 1, %	Initial composition 2, %	Composition 1 at t = 60 min	Composition 2 at t = 60 min
Fe_2O_3	9	9	1	1
Al	13	31	7	25
Al_2O_3	–	–	8	8
Ti_xAl_y	–	–	11	11
Al_zFe_t	–	–	3	3
Ti	68	50	60	42

we limit ourselves to the elasticity theory approximation. Let us generalise the relations between the components of the stress and strain tensors as follows

$$\sigma_{ij} = 2\mu\varepsilon_{ij} + \delta_{ij}\left[\lambda\varepsilon_{kk} - K\omega\right], \tag{25}$$

where in each phase

$$\omega = 3\sum_{k=1}^{n}\alpha_k\left(C_k - C_{k0}\right), \tag{26}$$

Hereinafter designations are taken as follows: $\mu = E/[2(1+\nu)]$, $\lambda = E\nu/[(1+\nu)(1-2\nu)]$ are Lamé coefficients, E is Young's modulus, ν is Poisson's ratio, $K = E/[3(1-2\nu)]$ is bulk elastic modulus; δ_{ij} is Kronecker delta (δ_{ij} = 1, if $i = j$; δ_{ij} = 0, if $i \neq j$), α_k are concentration expansion coefficients determined by the formulas

$$\alpha_k = \frac{1}{3V}\left(\frac{\partial V}{\partial C_k}\right). \tag{27}$$

Mechanical properties of all phases used in calculations are presented in Table 3.

In the case of a spherical particle the symmetry conditions allow us to consider

$$\sigma_{\theta r} = \sigma_{\theta\phi} = \sigma_{\phi r} = 0,$$

$$\varepsilon_{\theta r} = \varepsilon_{\theta\phi} = \varepsilon_{\phi r} = 0,$$

and the other components of the stress and strain tensors are functions only of the radial coordinate and time as a parameter. Under these circumstances:

Table 3. Properties of phases.

Phases	K, GPa	E, GPa	ν	ρ_k, g/cm^3	m_k, g/mole
Fe_2O_3	178.33	210	0.31	5.24	160
Al_2O_3	230	380	0.25	3.95	102
Fe_xAl_y	187	296	0.236	5.56	82.8
Al	75	70	0.34	2.7	27
Fe(Al)	85	87	0.33	3.47	82.2
$FeAl_2O_4$	172.4	153.8	0.35	4.3	173.8
TiO_2	210	250	0.28	4.23	80
Fe(Ti)	104	118	0.31	5.2	151.7
Fe_xTi_y	127	160	0.29	4.75	151.7
Ti_xAl_y	110	192.7	0.21	4.2	74.9
Ti	103.7	112	0.32	4.33	47.87
Fe+C	160	190	0.3	7.8	55.36

$$\varepsilon_{rr} = \frac{du}{dr}, \quad \varepsilon_{\theta\theta} = \varepsilon_{\phi\phi} = \frac{u}{r}. \tag{28}$$

Hence, in each phase we have the following equations relating stresses and displacements:

$$\sigma_{rr,k} = \frac{E_k}{1+\nu_k}\frac{du_k}{dr} + \frac{\nu_k E_k}{(1+\nu_k)(1-2\nu_k)}\left(\frac{du_k}{dr} + 2\frac{u_k}{r}\right) - \frac{E_k}{3(1-2\nu_k)}\omega_k,$$

$$\sigma_{\theta\theta,k} = \sigma_{\phi\phi,k} = \frac{E_k}{1+\nu_k}\frac{u_k}{r} + \frac{\nu_k E_k}{(1+\nu_k)(1-2\nu_k)}\left(\frac{du_k}{dr} + 2\frac{u_k}{r}\right) - \frac{E_k}{3(1-2\nu_k)}\omega_k.$$

In the spherical coordinate system, provided that the properties in phase do not depend on the coordinates, we obtain the equilibrium equation in the form of:

$$\frac{\partial\sigma_{rr}}{\partial r} + \frac{2\sigma_{rr} - \sigma_{\theta\theta} - \sigma_{\phi\phi}}{r} = 0. \tag{29}$$

Then for each phase we find:

$$\frac{d}{dr}\left[\frac{1}{r^2}\frac{d\left(r^2 u_k\right)}{dr}\right] = \frac{1}{3}\frac{1+\nu_k}{1-\nu_k}\frac{d\omega_k}{dr}. \tag{30}$$

Hence,

$$u_k = \frac{1}{3}\frac{1+\nu_k}{1-\nu_k}\frac{1}{r^2}\int_x^r \omega_k(r) r^2 dr + \frac{F_k}{3}r + \frac{H_k}{r^2}. \tag{31}$$

Here k = Fe_2O_3, Al_2O_3, Fe_xAl_y, Fe(Al), Al.

Expressions for the components of stress and strain tensors in each phase are as follows:

$$\sigma_{rr,k} = -\frac{2}{3}\frac{E_k}{1-\nu_k}\frac{1}{r^3}\int_{x_k}^r \omega_k(r) r^2 dr + \frac{1}{3}\frac{E_k}{1-2\nu_k}F_k - 2\frac{H_k}{r^3}\frac{E_k}{1+\nu_k},$$

$$\sigma_{\theta\theta,k} = \sigma_{\phi\phi,k} = \frac{1}{3}\frac{E_k}{1-\nu_k}\left[\frac{1}{r^3}\int_{x_k}^r \omega_k(r) r^2 dr - \omega_k(r)\right] + \frac{1}{3}\frac{E_k}{1-2\nu_k}F_k + \frac{H_k}{r^3}\frac{E_k}{1+\nu_k},$$

$$\varepsilon_{rr,k} = \frac{1+\nu_k}{1-\nu_k}\left(-\frac{2}{3}\frac{1}{r^3}\int_{x_k}^r \omega_k(r) r^2 dr + \frac{1}{3}\omega_k(r)\right) + \frac{F_k}{3} - 2\frac{H_k}{r^3},$$

$$\varepsilon_{\theta\theta,k} = \varepsilon_{\phi\phi,k} = \frac{1}{3}\frac{1+\nu_k}{1-\nu_k}\frac{1}{r^3}\int_{x_k}^r \omega_k(r) r^2 dr + \frac{F_k}{3} + \frac{H_k}{r^3}. \tag{32}$$

To determine the integration constants F_k and H_k, it is necessary to formulate the conditions at the interfaces. We assume that at all interfaces there are ideal contact conditions, which means that the radial components of the displacement vector and the radial components of the stress tensor are equal. In the center of the particle we have the symmetry condition

$$u_{Fe_2O_3} = 0,$$

at the boundary of the region we assume

$$\sigma_{rr,Al} = 0.$$

Substituting the obtained solution into the conditions at the boundaries, depending on the number of phases, we obtain systems of linear equations of different dimensionality. Since in the equilibrium problem the time included in the solution of the diffusion-kinetic problem is a parameter, knowing the position of the interface, we find the distribution of stress and strain components at given moments of time.

In the Cartesian coordinate system, the solution of the equilibrium problem of an object consisting of several layers differs from the one just considered. Thus, the equations of equilibrium in this case do not allow us to solve the problem. We assume that our multilayered object is a plate, unfastened and free from external forces. In these conditions we have:

$$\sigma_{xx} = \sigma_{xy} = \sigma_{xz} = \sigma_{yz} = 0,$$

$$\sigma_{zz} = \sigma_{yy} = \sigma(x).$$

From the compatibility equations there remain two equivalent equations

$$\varepsilon_{zz} = \varepsilon_{yy} = \varepsilon(x), \quad \frac{d^2\varepsilon}{dx^2} = 0. \tag{33}$$

Hence,

$$\varepsilon_{zz} = \varepsilon_{yy} = Nx + M. \tag{34}$$

From relations (25), we shall find:

$$\sigma_{zz} = \sigma_{yy} = \sigma = 2\mu\varepsilon + \left[\lambda\left(2\varepsilon + \varepsilon_{xx}\right) - K\omega\right],$$

$$\sigma_{xx} = 0 = 2\mu\varepsilon_{xx} + \left[\lambda\left(2\varepsilon + \varepsilon_{xx}\right) - K\omega\right].$$

The last equality gives:

$$\varepsilon_{xx} = \frac{\left[K\omega - 2\lambda\varepsilon\right]}{\lambda + 2\mu} = \frac{1}{3}\frac{1+\nu}{1-\nu}\omega - \frac{2\nu}{1-\nu}\varepsilon. \tag{35}$$

Therefore

$$\sigma = -\frac{\omega}{3}\frac{E}{1-\nu} + \frac{E}{1-\nu}(Nx + M). \tag{36}$$

These relations are true both for each phase separately and for the whole system. To find the integration constants N and M we use the integral equilibrium conditions [86].

For a free non-fixed plate (chip), the total force along the contour and the total moment of forces are equal to zero:

$$\int_0^{h_0} \sigma(x)\,dx = 0, \quad \int_0^{h_0} \sigma(x)\,x dx = 0. \tag{37}$$

The stress σ acts perpendicular to the plate contour in the yz plane, h_0 is total thickness of the plate.

Substituting the found expression (36) for stresses into the conditions (37), we find a system of linear equations for determining the integration constants

$$-\int_0^{h_0} \frac{\omega(x,t)}{3}\frac{E}{1-\nu}dx + N\int_0^{h_0} \frac{E}{1-\nu}x dx + M\int_0^{h_0} \frac{E}{1-\nu}dx = 0,$$

$$-\int_0^{h_0} \frac{\omega(x,t)}{3}\frac{E}{1-\nu}x dx + N\int_0^{h_0} \frac{E}{1-\nu}x^2 dx + M\int_0^{h_0} \frac{E}{1-\nu}x dx = 0.$$

Since the function $\omega(x,t)$ depends on the coordinates (on the area occupied by a particular phase) and the properties of the phases are different and may depend on the composition, all quantities remain under the integrals. Let us represent the last equations in the form

$$-I_1 + N\cdot I_2 + M\cdot I_3 = 0, \quad -J_1 + N\cdot J_2 + M\cdot I_2 = 0, \tag{38}$$

where

$$I_1 = -\int_0^{h_0} \frac{\omega(x,t)}{3}\frac{E}{1-\nu}dx, \quad J_1 = -\int_0^{h_0} \frac{\omega(x,t)}{3}\frac{E}{1-\nu}x dx,$$

$$I_2 = \int_0^{h_0} \frac{E}{1-\nu}x dx, \quad I_3 = \int_0^{h_0} \frac{E}{1-\nu}x dx, \quad J_2 = \int_0^{h_0} \frac{E}{1-\nu}x^2 dx.$$

The solution of the system (38) has the form:

$$N = \frac{J_1\cdot I_3 - I_1\cdot I_2}{J_2\cdot I_3 - I_2^2}, \quad M = \frac{J_1\cdot I_2 - I_1\cdot J_2}{J_2\cdot I_3 - I_2^2}. \tag{39}$$

Note that such problems are well known in the theory of thermoelasticity. Their solution methods are also simple and clear. The main problem here is related to the search for parameters and to the definition of functions $\omega_k(r)$, $\omega(x,t)$. However, since in the quasi-stationary approximation we obtain the concentration distributions in explicit form, some of the problems are eliminated.

For example, for the Al-Fe_2O_3 system with three formed phases (Al_2O_3, Fe_xAl_y and Fe(Al)) in the quasi-stationary approximation, the concentrations in the region of the particle material and matrix material are constant and equal to, respectively, 0 and 1 In other phases we have linear distributions.

According to the definition, in each phase in relations (25):

$$\omega_k = 3\sum_i \alpha_i^k \left(C_i^k - C_{i0}^k\right),$$

where k is the phase number, i is the component (diffusant) number.

If a single element diffuses, we omit the component index as above and leave only the phase designation, moving this index downwards. Then

$$\omega_k = 3\left[\alpha_D^k\left(C_D^k - C_{D0}^k\right) + \alpha_{ph}^k\left(C_{ph}^k - C_{ph0}^k\right)\right]$$
$$= 3\left(\alpha_D^k - \alpha_{ph}^k\right)\left(C_D^k - C_{D0}^k\right) \equiv \left(\alpha_k - \alpha_{k0}\right)\left(C_k - C_{k0}\right)$$

or

$$\omega_k = \left(\alpha_k - \alpha_{k0}\right)\left(C_k - C_{k0}\right), \tag{40}$$

where $\alpha_D^k \equiv \alpha_k$ is the concentration expansion coefficient of diffusant in the phase k, $\alpha_{ph}^k \equiv \alpha_{k0}$ is the effective coefficient of concentration expansion of the kth phase, $C_D^k = C_k$ is concentration of diffusant in kth phase, $C_D^k + C_{ph}^k = 1$.

The question arises: "How to estimate the concentration expansion coefficients?" In thermodynamic theory, these coefficients are defined similarly to thermal expansion coefficients and can be either adiabatic or isobaric:

$$\alpha_k = \frac{1}{3V}\left(\frac{\partial V}{\partial C_k}\right), \tag{41}$$

i.e., calculated or found at constant entropy or at constant pressure and temperature. This definition holds for any components of a homogeneous mixture. In this case

$$\alpha_k = \frac{1}{3}\left(\frac{w_k}{\sum_i w_i}\right), \quad (42)$$

where w_i is the molar volume of the component in the "own" phase (intrinsic molar volume).

In a heterogeneous (multiphase) system, each phase is in a constrained state, and in principle can border with any other phase, as well as with a crack or pore. Therefore, when estimating these coefficients, we shall assume that the phases are as if "smeared" throughout the local volume V, so that the definition remains valid, but the number of elementary components includes phases. Then for our system (in which the formation of a solution is taken into account) we write, for example, for aluminium

$$\alpha_{\mathrm{Al}} = \frac{1}{3}\left(\frac{w_{\mathrm{Al}}}{w_{\mathrm{Fe_2O_3}} + w_{\mathrm{Al_2O_3}} + w_{\mathrm{Fe_xAl_y}} + w_{\mathrm{Fe(Al)}} + w_{\mathrm{Al}}}\right),$$

where $w_k = m_k/\rho_k$. Thus, the defined coefficients will be different for the same system but with different phase sequence (Figs. 6a,b), i.e., they will formally take into account the presence of neighbours. This is shown in Table 4.

Since the solutions of diffusion-kinetic problems are known, the formulas for stresses can be written in the explicit form.

Thus, for the spherically symmetric problem for the variant shown in Fig. 6a from Eqs. (31) and (32) we find for the region occupied by iron oxide:

$$u_{\mathrm{Fe_2O_3}} = \frac{F_{\mathrm{Fe_2O_3}}}{3}r + \frac{H_{\mathrm{Fe_2O_3}}}{r^2},$$

$$\sigma_{rr,\mathrm{Fe_2O_3}} = \frac{1}{3}\frac{E_{\mathrm{Fe_2O_3}}}{1-2\nu_{\mathrm{Fe_2O_3}}}F_{Fe_2O_3} - 2\frac{H_{\mathrm{Fe_2O_3}}}{r^3}\frac{E_{\mathrm{Fe_2O_3}}}{1+\nu_{\mathrm{Fe_2O_3}}},$$

$$\sigma_{\theta\theta,\mathrm{Fe_2O_3}} = \sigma_{\phi\phi,\mathrm{Fe_2O_3}} = \frac{1}{3}\frac{E_{\mathrm{Fe_2O_3}}}{1-2\nu_{\mathrm{Fe_2O_3}}}F_{Fe_2O_3} + \frac{H_{\mathrm{Fe_2O_3}}}{r^3}\frac{E_{\mathrm{Fe_2O_3}}}{1+\nu_{\mathrm{Fe_2O_3}}},$$

$$\varepsilon_{rr,p} = \frac{F_{\mathrm{Fe_2O_3}}}{3} - 2\frac{H_{\mathrm{Fe_2O_3}}}{r^3},$$

$$\varepsilon_{\theta\theta,\mathrm{Fe_2O_3}} = \varepsilon_{\phi\phi,\mathrm{Fe_2O_3}} = \frac{F_{\mathrm{Fe_2O_3}}}{3} + \frac{H_{\mathrm{Fe_2O_3}}}{\xi^3}.$$

For the area occupied by aluminium:

$$u_{\mathrm{Al}} = \frac{F_{\mathrm{Al}}}{3}r + \frac{H_{\mathrm{Al}}}{r^2},$$

$$\sigma_{rr,\mathrm{Al}} = \frac{1}{3}\frac{E_{\mathrm{Al}}}{1-2\nu_{\mathrm{Al}}}F_{\mathrm{Al}} - 2\frac{H_{\mathrm{Al}}}{r^3}\frac{E_{\mathrm{Al}}}{1+\nu_{\mathrm{Al}}},$$

$$\sigma_{\theta\theta,\mathrm{Al}} = \sigma_{\phi\phi,\mathrm{Al}} = \frac{1}{3}\frac{E_{\mathrm{Al}}}{1-2\nu_{\mathrm{Al}}}F_{\mathrm{Al}} + \frac{H_{\mathrm{Al}}}{r^3}\frac{E_{\mathrm{Al}}}{1+\nu_{\mathrm{Al}}},$$

$$\varepsilon_{rr,\mathrm{Al}} = \frac{F_{\mathrm{Al}}}{3} - 2\frac{H_{\mathrm{Al}}}{r^3}, \quad \varepsilon_{\theta\theta,\mathrm{Al}} = \varepsilon_{\phi\phi,\mathrm{Al}} = \frac{F_{\mathrm{Al}}}{3} + \frac{H_{\mathrm{Al}}}{r^3}.$$

Table 4. Concentration expansion coefficients for the system Al-Fe_2O_3 with double oxide formation.

Phase	w_k, m³/mole	a_k for the scheme in Fig. 6a	a_k for the scheme in Fig. 6b
Al	$10\cdot10^{-6}$	0.029	0.025
Fe_2O_3	$30.47\cdot10^{-6}$	0.088	0.077
Al_2O_3	$36.4\cdot10^{-6}$	0.105	0.092
Fe_xAl_y	$14.89\cdot10^{-6}$	0.042	0.037
Fe(Al)	$14.89\cdot10^{-6}$	0.068	–
$FeAl_2O_4$	$40.42\cdot10^{-6}$	–	0.102

For each phase in the transition layer between Fe_2O_3 and Al (indices at the coefficients correspond to the designations in Fig. 6a):

$$u_k = \frac{1}{3}\frac{1+\nu_k}{1-\nu_k}\frac{1}{r^2}\int_{X_k}^{r}\omega_k(r)r^2dr + \frac{F_k}{3}r + \frac{H_k}{r^2},$$

$$\sigma_{rr,k} = -\frac{2}{3}\frac{E_k}{1-\nu_k}\frac{1}{r^3}\int_{X_k}^{r}\omega_k(r)r^2dr + \frac{1}{3}\frac{E_k}{1-2\nu_k}F_k - 2\frac{H_k}{r^3}\frac{E_k}{1+\nu_k},$$

$$\sigma_{\theta\theta,k} = \sigma_{\phi\phi,k} = \frac{1}{3}\frac{E_k}{1-\nu_k}\left[\frac{1}{r^3}\int_{X_k}^{r}\omega_k(r)r^2dr - \omega_k(r)\right] + \frac{1}{3}\frac{E_k}{1-2\nu_k}F_k + \frac{H_k}{r^3}\frac{E_k}{1+\nu_k},$$

$$\varepsilon_{rr,k} = \frac{1+\nu_k}{1-\nu_k}\left(-\frac{2}{3}\frac{1}{r^3}\int_{X_k}^{r}\omega_k(r)r^2dr + \frac{1}{3}\omega_k(r)\right) + \frac{F_k}{3} - 2\frac{H_k}{r^3},$$

$$\varepsilon_{\theta\theta,k} = \varepsilon_{\phi\phi,k} = \frac{1}{3}\frac{1+\nu_k}{1-\nu_k}\frac{1}{r^3}\int_{X_k}^{r}\omega_k(r)r^2dr + \frac{F_k}{3} + \frac{H_k}{r^3},$$

$$\int_{X_k}^{r}\omega_k(r)r^2dr \equiv 3(\alpha_k - \alpha_{k0})\int_{X_k}^{r}C_k(r)r^2dr,$$

where $\omega_k(r)$ follows from Eq. (40), and $C_k(r)$ is from Eq. (14).

Since the interfaces are functions of time and time is an external parameter in this problem, the integrals from the concentrations are easily taken

$$I_k = \int_{X_k}^{r}C_k(r)r^2dr = -\frac{A_k}{2}\left(r^2 - X_k^{\,2}\right) + \frac{B_k}{3}\left(r^3 - X_k^{\,3}\right). \quad (43)$$

The integration constants F_k, H_k for each region are determined from the boundary conditions, which we choose as ideal contact conditions, i.e., the radial components of the displacement vector and stress tensor are continuous at the interface. In the center, the symmetry condition is satisfied, and on the outer boundary of the region (reaction cell) either no load is applied or displacements are forbidden. For the

scheme in Fig. 6a (with solution formation) we have 10 equations for determining 10 integration constants:

$$r = 0: \quad H_{\mathrm{Fe_2O_3}} = 0;$$

$$r = X_1: \quad \frac{F_{\mathrm{Fe_2O_3}}}{3} X_1^{\,3} = \frac{F_1}{3} X_1^{\,3} + H_1,$$

$$\frac{1}{3}\frac{E_{\mathrm{Fe_2O_3}}}{1-2\nu_{\mathrm{Fe_2O_3}}} F_{\mathrm{Fe_2O_3}} X_1^{\,3} = \frac{1}{3}\frac{E_{\mathrm{Al_2O_3}}}{1-2\nu_{\mathrm{Al_2O_3}}} F_1 X_1^{\,3} - 2H_1 \frac{E_{\mathrm{Al_2O_3}}}{1+\nu_{\mathrm{Al_2O_3}}};$$

$$r = R_p: \quad \frac{1}{3}\frac{1+\nu_{\mathrm{Al_2O_3}}}{1-\nu_{\mathrm{Al_2O_3}}} 3(\alpha_1 - \alpha_{10}) I_1(R_p) + \frac{F_1}{3} R_p^{\,3} + H_1 = \frac{F_2}{3} R_p^{\,3} + H_2,$$

$$-\frac{2}{3}\frac{E_{\mathrm{Al_2O_3}}}{1-\nu_{\mathrm{Al_2O_3}}} 3(\alpha_1 - \alpha_{10}) I_1(R_p) + \frac{1}{3}\frac{E_{\mathrm{Al_2O_3}}}{1-2\nu_{\mathrm{Al_2O_3}}} F_1 R_p^{\,3} - 2H_1 \frac{E_{\mathrm{Al_2O_3}}}{1+\nu_{\mathrm{Al_2O_3}}} = \frac{1}{3}\frac{E_{\mathrm{Fe_xAl_y}}}{1-2\nu_{\mathrm{Fe_xAl_y}}} F_2 R_p^{\,3} - 2H_2 \frac{E_{\mathrm{Fe_xAl_y}}}{1+\nu_{\mathrm{Fe_xAl_y}}};$$

$$r = X_2: \quad \frac{1}{3}\frac{1+\nu_{\mathrm{Fe_xAl_y}}}{1-\nu_{\mathrm{Fe_xAl_y}}} 3(\alpha_2 - \alpha_{20}) I_2(_2) + \frac{F_2}{3} X_2^{\,3} + H_2 = \frac{F_3}{3} X_2^{\,3} + H_3,$$

$$-\frac{2}{3}\frac{E_{\mathrm{Fe_xAl_y}}}{1-\nu_{\mathrm{Fe_xAl_y}}} 3(\alpha_2 - \alpha_{20}) I_2(X_2) + \frac{1}{3}\frac{E_{\mathrm{Fe_xAl_y}}}{1-2\nu_{\mathrm{Fe_xAl_y}}} F_2 X_2^{\,3} - 2H_2 \frac{E_{\mathrm{Fe_xAl_y}}}{1+\nu_{\mathrm{Fe_xAl_y}}} = \frac{1}{3}\frac{E_{\mathrm{Fe(Al)}}}{1-2\nu_{\mathrm{Fe(Al)}}} F_3 X_2^{\,3} - 2H_3 \frac{E_{\mathrm{Fe(Al)}}}{1+\nu_{\mathrm{Fe(Al)}}};$$

$$r = X_3: \quad \frac{1}{3}\frac{1+\nu_{\mathrm{Fe(Al)}}}{1-\nu_{\mathrm{Fe(Al)}}} 3(\alpha_3 - \alpha_{30}) I_3(X_3) + \frac{F_3}{3} X_3^{\,3} + H_3 = \frac{F_{\mathrm{Al}}}{3} X_3^{\,3} + H_{\mathrm{Al}},$$

$$-\frac{2}{3}\frac{E_{\mathrm{Fe(Al)}}}{1-\nu_{\mathrm{Fe(Al)}}} 3(\alpha_3 - \alpha_{30}) I_3(X_3) + \frac{1}{3}\frac{E_{\mathrm{Fe(Al)}}}{1-2\nu_{\mathrm{Fe(Al)}}} F_3 X_3^{\,3} - 2H_3 \frac{E_{\mathrm{Fe(Al)}}}{1+\nu_{\mathrm{Fe(Al)}}} = \frac{1}{3}\frac{E_{\mathrm{Al}}}{1-2\nu_{\mathrm{Al}}} F_{\mathrm{Al}} X_3^{\,3} - 2H_{\mathrm{Al}} \frac{E_{\mathrm{Al}}}{1+\nu_{\mathrm{Al}}};$$

$$r = R_m: \quad \frac{R_m^3}{3} F_{\mathrm{Al}} + H_{\mathrm{Al}} = 0.$$

Here

$$I_1(R_p) = -\left[\frac{A_1\left(R_p^{\,2} - X_1^{\,2}\right)}{2} - \frac{B_1\left(R_p^{\,3} - X_1^{\,3}\right)}{3}\right],$$

$$I_2(X_2) = -\left[\frac{A_2\left(X_2^{\,2} - R_p^{\,2}\right)}{2} - \frac{B_2\left(X_2^{\,3} - R_p^{\,3}\right)}{3}\right],$$

$$I_3(X_3) = -\left[\frac{A_3\left(X_3^{\,2} - X_2^{\,2}\right)}{2} - \frac{B_3\left(X_3^{\,3} - X_2^{\,3}\right)}{3}\right].$$

This equation system can, of course, be solved exactly. However, to avoid errors, for problems with more than two new phases, it is better to apply any convenient numerical method.

In the Cartesian coordinate system, everything is much simpler, as it is required to find only two integration constants in the equilibrium problem. However, cumbersome coefficients appear. For the scheme shown in Fig. 6a, in Eqs. (38), under the condition of constant phase properties, we have

$$I_1 = \int_{X_1}^{h_1} \frac{\omega_1(x,t)}{3}\frac{E_{\mathrm{Al_2O_3}}}{1-\nu_{\mathrm{Al_2O_3}}}dx + \int_{h_1}^{X_2} \frac{\omega_2(x,t)}{3}\frac{E_{\mathrm{Fe_xAl_y}}}{1-\nu_{\mathrm{Fe_xAl_y}}}dx + \int_{X_2}^{X_3} \frac{\omega_3(x,t)}{3}\frac{E_{\mathrm{Fe(Al)}}}{1-\nu_{\mathrm{Fe(Al)}}}dx,$$

$$I_2 = \frac{E_{\mathrm{Fe_2O_3}}}{1-\nu_{\mathrm{Fe_2O_3}}}\frac{X_1^2}{2} + \frac{E_{\mathrm{Al_2O_3}}}{1-\nu_{\mathrm{Al_2O_3}}}\left(\frac{h_1^2}{2} - \frac{X_1^2}{2}\right) + \frac{E_{\mathrm{Fe_xAl_y}}}{1-\nu_{\mathrm{Fe_xAl_y}}}\left(\frac{X_2^2}{2} - \frac{h_1^2}{2}\right) + \frac{E_{\mathrm{Fe(Al)}}}{1-\nu_{\mathrm{Fe(Al)}}}\left(\frac{X_3^2}{2} - \frac{X_2^2}{2}\right) + \frac{E_{\mathrm{Al}}}{1-\nu_{\mathrm{Al}}}\left(\frac{h_0^2}{2} - \frac{X_3^2}{2}\right),$$

$$I_3 = \frac{E_{\mathrm{Fe_2O_3}}}{1-\nu_{\mathrm{Fe_2O_3}}} X_1 + \frac{E_{\mathrm{Al_2O_3}}}{1-\nu_{\mathrm{Al_2O_3}}}(h_1 - X_1) + \frac{E_{\mathrm{Fe_xAl_y}}}{1-\nu_{\mathrm{Fe_xAl_y}}}(X_2 - h_1) + \frac{E_{\mathrm{Fe(Al)}}}{1-\nu_{\mathrm{Fe(Al)}}}(X_3 - X_2) + \frac{E_{\mathrm{Al}}}{1-\nu_{\mathrm{Al}}}(h_0 - X_3),$$

$$J_1 = \int_{X_1}^{h_1} \frac{\omega_1(x,t)}{3}\frac{E_{\mathrm{Al_2O_3}}}{1-\nu_{\mathrm{Al_2O_3}}}x\,dx + \int_{h_1}^{X_2} \frac{\omega_2(x,t)}{3}\frac{E_{\mathrm{Fe_xAl_y}}}{1-\nu_{\mathrm{Fe_xAl_y}}}x\,dx + \int_{X_2}^{X_3} \frac{\omega_3(x,t)}{3}\frac{E_{\mathrm{Fe(Al)}}}{1-\nu_{\mathrm{Fe(Al)}}}x\,dx,$$

$$J_2 = \frac{E_{\mathrm{Fe_2O_3}}}{1-\nu_{\mathrm{Fe_2O_3}}}\frac{X_1^3}{3} + \frac{E_{\mathrm{Al_2O_3}}}{1-\nu_{\mathrm{Al_2O_3}}}\left(\frac{h_1^3}{3} - \frac{X_1^3}{3}\right) + \frac{E_{\mathrm{Fe_xAl_y}}}{1-\nu_{\mathrm{Fe_xAl_y}}}\left(\frac{X_2^3}{3} - \frac{h_1^3}{3}\right) + \frac{E_{\mathrm{Fe(Al)}}}{1-\nu_{\mathrm{Fe(Al)}}}\left(\frac{X_3^3}{3} - \frac{X_2^3}{3}\right) + \frac{E_{\mathrm{Al}}}{1-\nu_{\mathrm{Al}}}\left(\frac{h_0^3}{3} - \frac{X_3^3}{3}\right).$$

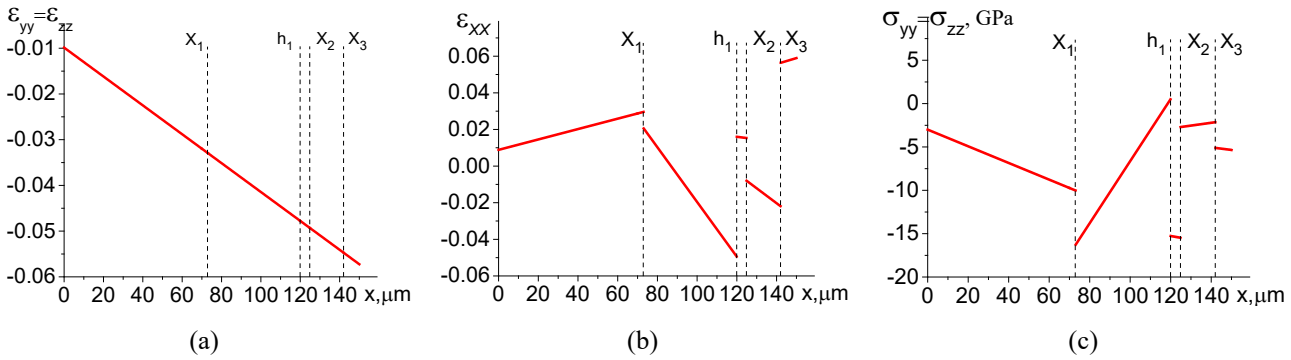

Fig. 12. Distributions of strain (a,b) and stresses (c) tensor components at the time $t = 400$ s during the formation of phases in the Fe_2O_3-Al system according to the scheme shown in Fig. 6a.

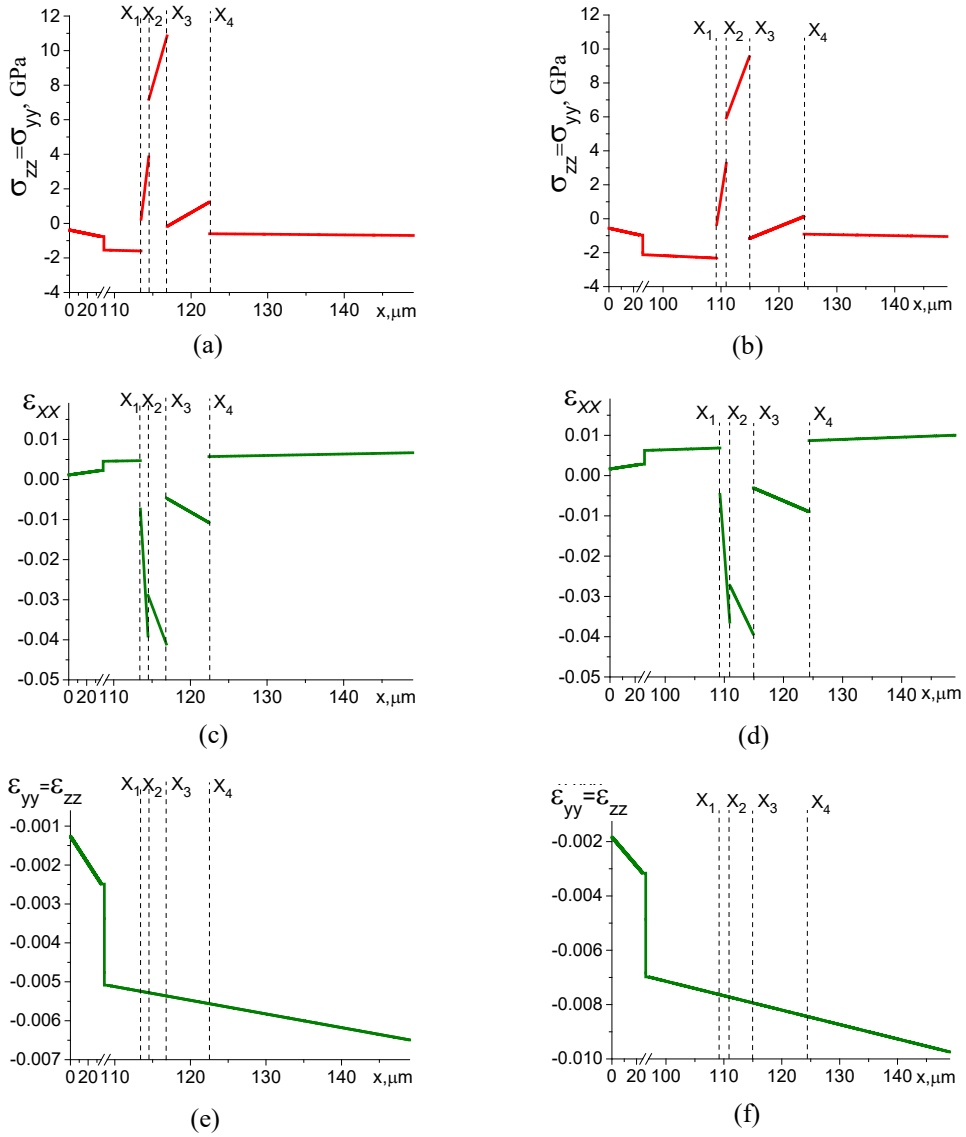

Fig. 13. Distributions of stress (a,b) and strain (c,d,e,f) tensor components at the time moments $t = 100$ s (left) and $t = 400$ s (right) during the formation of phases in the Fe_2O_3-Al system according to the scheme shown in Fig. 6b.

An example of strain and stress distribution for the moment of time $t = 400$ s, the same as for the concentration distribution in Fig. 7, is given in Fig. 12. Since the concentration distributions are linear in the Cartesian coordinate system, the mechanical quantities are distributed linearly along the coordinate. The strains are small and the stresses in the *yz* plane are discontinuous, which does not contradict the continuity of stresses in the *x* direction ($\sigma_{xx} = 0$). The

Table 5. Concentration expansion coefficients for the system Ti-Fe_2O_3.

Phase	w_{ph}, m^3/mole	a_k
Fe_2O_3	$30.47\cdot10^{-6}$	0.084
TiO_2	$18.9\cdot10^{-6}$	0.052
Fe_xTi_y	$30.93\cdot10^{-6}$	0.085
Fe(Ti)	$29.17\cdot10^{-6}$	0.081
Ti	$10.6\cdot10^{-6}$	0.029

maximum stresses occur in the aluminium oxide region. Very high stress values have been obtained by other authors in similar calculations (references are given above).

In the case of the scheme shown in Fig. 6b, the situation is similar (Fig. 13). The maximum stresses also take place in the Al_2O_3 region. However, the stresses are higher due to a different phase composition. With the passage of time, i.e. with the increase of the size of the growing phases, the maximum stresses decrease, which is also noticeable in the figures. The formulas for calculating stresses and strains are obtained in a similar way and are not presented here.

Calculation of stresses and strains for the Ti-Fe_2O_3 system is carried out similarly. The required mechanical properties are given in Table 3. The concentration expansion coefficients are given in Table 5. The calculation for Fig. 14 is made for different compositions of the initial mixtures and corresponds to the concentration distributions in Fig. 9. Examples of calculations for the spherical coordinate system are given in Ref. [87].

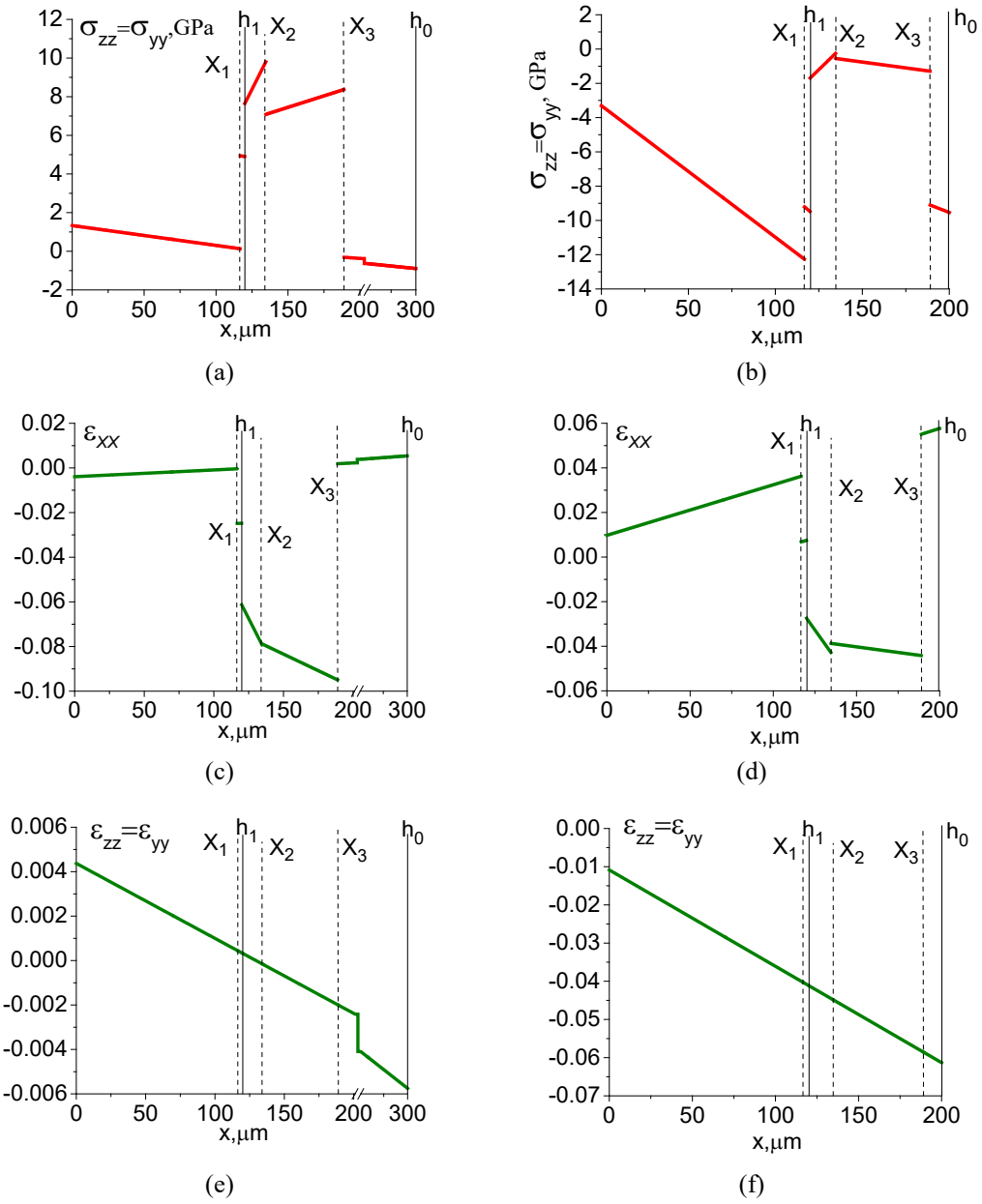

Fig. 14. Distributions of stress (a,b) and strain (c,d,e,f) tensor components at the time t = 80 s for different initial compositions of Fe_2O_3-Ti system: on the left – iron oxide volume fraction is 0.4; on the right – 0.6.

Table 6. Concentration expansion coefficients for the system Ti-Al-Fe_2O_3-(Fe+C).

Phase	w_{ph}, m³/mole	a_k
Al	$10\cdot10^{-6}$	0.026
Al_zFe_t	$14.89\cdot10^{-6}$	0.039
Al_2O_3	$36.4\cdot10^{-6}$	0.095
Fe_2O_3	$30.47\cdot10^{-6}$	0.08
Ti_xAl_y	$17.83\cdot10^{-6}$	0.046
Ti	$10.6\cdot10^{-6}$	0.028
Fe+C	$7.1\cdot10^{-6}$	0.018

For the ternary system (Fig. 10) in the Cartesian coordinate system, the concentration distribution has the form (16). Since six regions are involved in the calculation, the total solution of the diffusion problem contains 12 coefficients [39]. Stresses and strains are calculated by formulas (32)–(34), where integrals involved in the formulae for coefficients (39) are

$$I_1 = \int_{X_4}^{X_2} \frac{\omega_5(x,t)}{3}\frac{E_{\mathrm{Ti}_x\mathrm{Al}_y}}{1-\nu_{\mathrm{Ti}_x\mathrm{Al}_y}}dx + \int_{X_1}^{h_1-\delta} \frac{\omega_2(x,t)}{3}\frac{E_{\mathrm{Fe}_x\mathrm{Al}_y}}{1-\nu_{\mathrm{Fe}_x\mathrm{Al}_y}}dx + \int_{h_1-\delta}^{X_3} \frac{\omega_3(x,t)}{3}\frac{E_{\mathrm{Al_2O_3}}}{1-\nu_{\mathrm{Al_2O_3}}}dx,$$

$$I_2 = \frac{E_{\mathrm{Ti}}}{1-\nu_{\mathrm{Ti}}}\left(\frac{X_4^2}{2}-\frac{h_2^2}{2}\right)+\frac{E_{\mathrm{Ti}_x\mathrm{Al}_y}}{1-\nu_{\mathrm{Ti}_x\mathrm{Al}_y}}\left(\frac{X_2^2}{2}-\frac{X_4^2}{2}\right) + \frac{E_{\mathrm{Al}}}{1-\nu_{\mathrm{Al}}}\left(\frac{X_1^2}{2}-\frac{X_2^2}{2}\right)+\frac{E_{\mathrm{Fe}_x\mathrm{Al}_y}}{1-\nu_{\mathrm{Fe}_x\mathrm{Al}_y}}\left(\frac{(h_1-\delta)^2}{2}-\frac{X_1^2}{2}\right) + \frac{E_{\mathrm{Al_2O_3}}}{1-\nu_{\mathrm{Al_2O_3}}}\left(\frac{X_3^2}{2}-\frac{(h_1-\delta)^2}{2}\right)+\frac{E_{\mathrm{Fe_2O_3}}}{1-\nu_{\mathrm{Fe_2O_3}}}\left(\frac{h_1^2}{2}-\frac{X_3^2}{2}\right) + \frac{E_{\mathrm{Fe(C)}}}{1-\nu_{\mathrm{Fe(C)}}}\left(\frac{h_0^2}{2}-\frac{h_1^2}{2}\right),$$

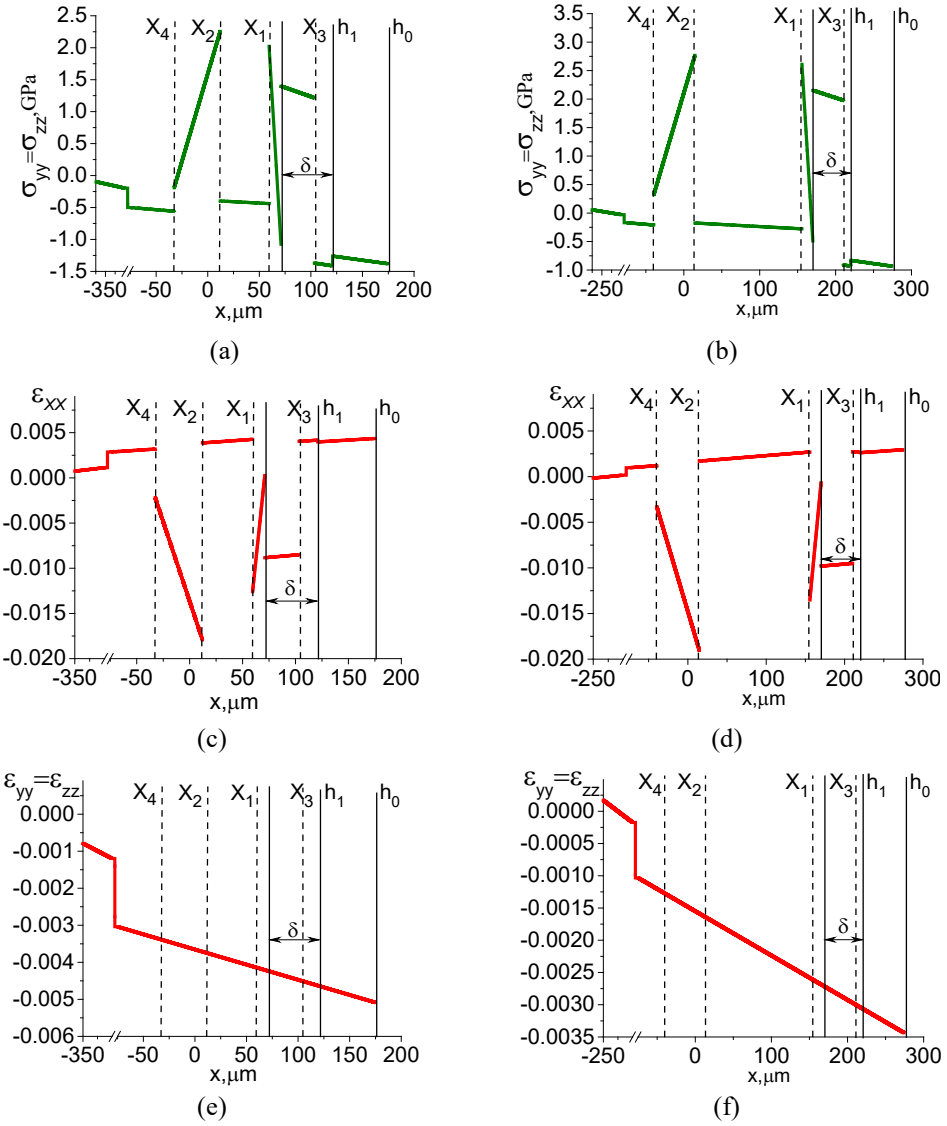

Fig. 15. Distribution of stresses (a,b) and strains (c,d,e,f) in the system Ti-Al-Fe_2O_3-(Fe+C) during phase formation at the time t = 50 min for different compositions presented in Table 2: Composition No.1 (left) and composition No.2 (right).

$$I_3 = \frac{E_{\mathrm{Ti}}}{1-\nu_{\mathrm{Ti}}}\left(X_4 - h_2\right) + \frac{E_{\mathrm{Ti}_x\mathrm{Al}_y}}{1-\nu_{\mathrm{Ti}_x\mathrm{Al}_y}}\left(X_2 - X_4\right) + \frac{E_{\mathrm{Al}}}{1-\nu_{\mathrm{Al}}}\left(X_1 - X_2\right) + \frac{E_{\mathrm{Fe}_x\mathrm{Al}_y}}{1-\nu_{\mathrm{Fe}_x\mathrm{Al}_y}}\left(\left(h_1 - \delta\right) - X_1\right) + \frac{E_{\mathrm{Al_2O_3}}}{1-\nu_{\mathrm{Al_2O_3}}}\left(X_3 - \left(h_1 - \delta\right)\right) + \frac{E_{\mathrm{Fe_2O_3}}}{1-\nu_{\mathrm{Fe_2O_3}}}\left(h_1 - X_3\right) + \frac{E_{\mathrm{Fe(C)}}}{1-\nu_{\mathrm{Fe(C)}}}\left(h_0 - h_1\right),$$

$$J_1 = \int_{X_4}^{X_2} \frac{\omega_5\left(x,t\right)}{3}\frac{E_{\mathrm{Ti}_x\mathrm{Al}_y}}{1-\nu_{\mathrm{Ti}_x\mathrm{Al}_y}}xdx + \int_{X_1}^{h_1-\delta} \frac{\omega_2\left(x,t\right)}{3}\frac{E_{\mathrm{Fe}_x\mathrm{Al}_y}}{1-\nu_{\mathrm{Fe}_x\mathrm{Al}_y}}xdx + \int_{h_1-\delta}^{X_3} \frac{\omega_3\left(x,t\right)}{3}\frac{E_{\mathrm{Al_2O_3}}}{1-\nu_{\mathrm{Al_2O_3}}}xdx,$$

$$J_2 = \frac{E_{\mathrm{Ti}}}{1-\nu_{\mathrm{Ti}}}\left(\frac{X_4^3}{3} - \frac{h_2^3}{3}\right) + \frac{E_{\mathrm{Ti}_x\mathrm{Al}_y}}{1-\nu_{\mathrm{Ti}_x\mathrm{Al}_y}}\left(\frac{X_2^3}{3} - \frac{X_4^3}{3}\right) + \frac{E_{\mathrm{Al}}}{1-\nu_{\mathrm{Al}}}\left(\frac{X_1^3}{3} - \frac{X_2^3}{3}\right) + \frac{E_{\mathrm{Fe}_x\mathrm{Al}_y}}{1-\nu_{\mathrm{Fe}_x\mathrm{Al}_y}}\left(\frac{\left(h_1-\delta\right)^3}{3} - \frac{X_1^3}{3}\right) + \frac{E_{\mathrm{Al_2O_3}}}{1-\nu_{\mathrm{Al_2O_3}}}\left(\frac{X_3^3}{3} - \frac{\left(h_1-\delta\right)^3}{3}\right) + \frac{E_{\mathrm{Fe_2O_3}}}{1-\nu_{\mathrm{Fe_2O_3}}}\left(\frac{h_1^3}{3} - \frac{X_3^3}{3}\right) + \frac{E_{\mathrm{Fe(C)}}}{1-\nu_{\mathrm{Fe(C)}}}\left(\frac{h_0^3}{3} - \frac{h_1^3}{3}\right).$$

The properties of the phases are given in Table 3, and the concentration expansion coefficients for this system are given in Table 6. In this case, the maximum strains are observed in the intermetallic phases Ti_xAl_y and Al_zFe_t (Fig. 15). The strains in the phases, as above, are both compressive and tensile, which is directly related to the different properties of the phases. Different variants of volume changes in sintering processes associated with stresses and strains of different nature are discussed, for example, in Ref. [88]. Composition 2 (see Table 2) is characterised by higher stresses than composition 1 during phase growth, as well as by lower strain values.

4. CONCLUSION

Thus, in the present work we have recalled the basic ideas of the theory of reactive diffusion and variants for stresses estimation in the diffusion zone in different applications. We have given examples of particular problems modelling phase formation in local volumes of the complex system Ti-Al-Fe_2O_3-Fe. We have presented solutions of partial problems of reaction diffusion theory in the quasi-stationary approximation and have shown that this approach can be extended to rather complicated situations. In the calculation of stresses associated with diffusion and phase formation, the quasi-stationary approach allowed us to write out formulas for stresses and strains in explicit form, which is convenient in those cases where the calculation of stresses is an intermediate step in the solution of problems. As a result, general formulas for stresses and strains for a multiphase system in spherical and Cartesian coordinate systems have been derived, which may be useful for other applications.

Note, that in this review the mechanisms of mutual diffusion in phases [89], and also variants of problems with formation of several intermediate phases [90] were not analysed. However, the methods used in the paper are applicable in these cases as well.

ACKNOWLEDGMENTS

The work was supported by the Russian Science Foundation and the Tomsk Region Administration under grant No. 22-13-20031, https://rscf.ru/project/22-13-20031/.

REFERENCES

[1] E.N. Korosteleva, A.G. Knyazeva, I.O. Nikolaev, Phase Formation in Reactive Sintering with Reduction, *Phys. Mesomech*., 2023, vol. 26, pp. 39–47.

[2] M. Anisimova, A. Knyazeva, Basic models of phase formation at the mesolevel under reactive sintering of Ti-Al-Fe_2O_3 powder mixture, in: D. Sorokin, A. Grishkov (Eds.), *Proceeding of 8th International Congress on Energy Fluxes and Radiation Effects (EFRE 2022)*, Institute of High Current Electronics SB RAS, HCEI SB RAS, 2022.

[3] E.L. Shvedkov, E.T. Denisenko, Kovensky I.I., *Slovar-spravochnik po poroshkovoy metallurgii* [Dictionary-handbook of powder metallurgy], Naukova dumka Publ., Kyiv, 1982 (in Russian).

[4] M. Kizilyalli, J. Corish, R. Metselaar, Definitions of terms for diffusion in the solid state, *Pure Appl. Chem.*, 1999, vol. 71, no. 7, pp. 1307–1325.

[5] V.N. Chebotin, *Chemical diffusion in solids*, Nauka, Moscow, 1989 (in Russian).

[6] V.I. Dybkov, *Solid state reaction kinetics*, IPMS Publications, Kyev, 2013.

[7] A.M. Gusak, T.V. Zaporozhets, Y.O. Lyashenko, S.V. Kornienko, M.O. Pasichnyy, A.S. Shirinyan, *Diffusion-Controlled Solid State Reactions: In Alloys, Thin-Films, and Nanosystems*, John Wiley and Sons, New York, 2010.

[8] J. Svoboda, F.D Fischer, A new computational treatment of reactive diffusion in binary systems, *Comput. Mater. Sci.*, 2013, vol. 78, pp. 39–46.

[9] Y.M. Grigor'ev, S.L. Kharatyan, Z.S.Andrianova, A.N. Ivanova, A.G. Merzhanov, Diffusion kinetics of interaction of metals with gases, *Combust. Explos. Shock Waves*, 1977, vol. 13, pp. 604–610.

[10] Y.M. Grigor'ev, S.L. Kharatyan, Z.S. Andrianova, A.N. Ivanova, A.G. Merzhanov, Theory of reaction diffusion for bodies of plane, cylindrical, and spherical symmetry, *J. Eng. Phys.*, 1977, vol. 33, pp. 1353–1358.

[11] J. Benar, *Oxidation of Metals*, Metallurgiya, Moscow, 1968 (in Russian).

[12] J. Svoboda, F.D. Fischer, P. Fratzl, Diffusion and creep in multi-component alloys with non-ideal sources and

sinks for vacancies, *Acta Mater*., 2006, vol. 54, no. 11, pp. 3043–3053.

[13] K.P. Gurov, E.A. Smirnov, A.N. Shabalin, *Diffuziya i kinetika fazovykh prevrashcheniy v metallakh i splavakh* [Diffusion and kinetics of phase transformations in metals and alloys], MEPHI, Moscow, 1990 (in Russian).

[14] B.Ya. Lyubov, *Kinetic Theory of Phase Transformations*, Amerind Pub., New Delhi, 1978.

[15] G.D.C. Kuiken, *Thermodynamics of irreversible processes. Applicationa to diffusion and rheology*, J. Wiley and Sons, Chichester, 1994.

[16] I. Kaur, W. Gust. *Fundamentals of Grain and Interphase Boundary Diffusion*, Ziegler Press, Stuttgart, 1989.

[17] Y.L. Corcoran, A.H. King, N. de Lanerolle, B. Kim, Grain Boundary Diffusion Layers on Silicon and Growth of Titanium Silicide, *J. Electron. Mater.*, 1990, vol.19, pp. 1177–1183.

[18] H.H. Farrell, G.H. Glimer, M. Suenaga, Grain boundary diffusion and growth of intermetallic layers, *J. Appl. Phys.*, 1974, vol. 45, no. 9, pp. 4025–4035.

[19] A. Furuto, M. Kajihara, Numerical Analysis for Kinetics of Reactive Diffusion Controlled by Boundary and Volume Diffusion in a Hypothetical Binary System, *Mater. Trans.*, 2008, vol. 49, no. 2, pp. 294-303.

[20] D.L. Bekea, Yu. Kaganovskii, G.L. Katona, Interdiffusion along grain boundaries – Diffusion induced grain boundary migration, low temperature homogenization and reactions in nanostructured thin films, *Prog. Mater. Sci.*, 2018, vol. 98, pp. 625–674.

[21] A.M. Gusak, Flux-Driven Lateral Grain Growth during Reactive Diffusion, *Metallofiz. Noveishie Tekhnol.*, 2020, vol. 42, no. 10, pp. 1335–1346.

[22] M.V. Chepak-Gizbrekht, A.G. Knyazeva, Two-dimensional model of grain boundary diffusion and oxidation, *PNRPU Mechanics Bulletin*, 2022, no. 1, pp. 156–166.

[23] M.V. Chepak-Gizbrekht, A.G. Knyazeva, Oxidation of TiAl alloy by oxygen grain boundary diffusion, *Intermetallics*, 2023, vol. 162, art. no. 107993.

[24] M.V. Chepak-Gizbrekht, A.G. Knyazeva, Modeling the oxidation process of TiAl and Ti_3Al intermetallic compounds due to grain-boundary diffusion of oxygen, *Uchenye Zapiski Kazanskogo Universiteta. Seriya Fiziko-Matematicheskie Nauki*, 2023, vol. 165, no 3, pp. 307-321 (in Russian).

[25] A. Knyazeva, O. Kryukova, A. Maslov, Two-level model of the grain boundary diffusion under electron beam action, *Comput. Mater. Sci*., 2021, vol. 196, art. no. 110548.

[26] G. Wang, B. Gleeson, D.L. Douglass, Phenomenological Treatment of Multilayer Growth, *Oxid Met*., 1989, vol. 31, no. 5–6, pp. 415–429.

[27] B. Cockeram, G. Wang, The influence of multi-layered kinetics on the selection of the primary phase during the diffusion-controlled growth of titanium-silicide layers, *Thin Solid Films*, 1995, vol. 269, no. 1–2, pp. 57–63.

[28] G.-X. Li, C.W. Powell, Theory of reaction diffusion in binary systems, *Acta Metall*., 1985, vol. 33, no. 1, pp. 23–31.

[29] V.I. Dybkov, Reaction diffusion in binary solid-solid, solid-liquid and solid-gaz sestems: common and distinctive features, *Defect Diffus Forum*, 2001, vol. 194–199, pp. 1503–1533.

[30] U. Gösele; K.N. Tu, "Critical thickness" of amorphous phase formation in binary diffusion couples, *J. Appl. Phys.*, 1989, vol. 66, no. 6, pp. 2619–2626.

[31] M. Kajihara, Influence of Temperature Dependence of Solubility on Kinetics for Reactive Diffusion in a Hypothetical Binary System, *Mater. Trans.*, 2008, vol. 49, no. 4, pp. 715–722.

[32] M. Kajihara, Analysis of kinetics of reactive diffusion in a hypothetical binary system, *Acta Mater*., 2004, vol. 52, no. 5, pp. 1193–1200.

[33] M. Danielewski, B. Wierzba, A. Gusak, M. Pawełkiewicz, J. Janczak-Rusch, Chemical interdiffusion in binary systems; interface barriers and phase competition, *J. Appl. Phys.*, 2011, vol. 110, no. 12, art. no. 123705.

[34] J. Svoboda, F.D. Fischer, Incorporation of vacancy generation/annihilation into reactive diffusion concept – Prediction of possible Kirkendall porosity, *Comput. Mater. Sci.*, 2017, vol. 127, pp. 136–140.

[35] A.V. Nazarov, K.P. Gurov. Kinetic theory of mutual diffusion in a binary system. Concentration of vacancies during mutual diffusion, *The Physics of Metals and Metallography*, 1974, vol. 37, no. 3, pp. 41–47.

[36] Yu.E. Ugaste, Kinetics of phase growth during mutual diffusion in multiphase binary systems, *Physics and Chemistry of Materials Treatment*, 1979, no. 3, pp.125–131 (in Russian).

[37] A.G. Knyazeva, M.A. Anisimova, E.N. Korosteleva, Features of diffusion-controlled processes of regulated volumetric synthesis from powder mixtures Ti–Al–Fe–Fe_2O_3, *PNRPU Mechanics Bulletin*, 2022, no. 3, pp. 125–134.

[38] E.N. Korosteleva, A.G.Knyazeva, M.A. Anisimova, I.O. Nikolaev, The impact of impurities on the Al–Fe–C system phase composition changes during sintering, *Powder Metallurgy and Functional Coatings*, 2023, vol. 17, no. 2, pp. 5–13.

[39] M.A. Anisimova, A.G.Knyazeva, E.N. Korosteleva, I.O. Nikolaev, Phase formation during composite synthesis under conditions of reactive sintering of the Ti+Al+Fe_2O_3+(Fe+C) powder mixture, *Izvestiya Vuzov. Fizika*, 2023, vol. 66, no 11, pp. 7–16 (in Russian).

[40] Y. Zhao, Y. Chen, S. Ai, D. Fang, A diffusion, oxidation reaction and large viscoelastic deformation coupled model with applications to SiC fiber oxidation, *Int. J. Plast.*, 2019, vol. 118, pp. 173–189.

[41] B.E. Deal, A.S. Grove, General relationship for the thermal oxidation of silicon, *J. Appl. Phys.*, 1965, vol.36, no. 12, pp. 3770–3778.

[42] M. Wilson, E. Opila, A review of SiC fiber oxidation with a new study of Hi-Nicalon SiC fiber oxidation, *Adv. Eng. Mater*., 2016, vol. 18, no. 10, pp. 1698–1709.

[43] W.L. Wang, S. Lee; J.R. Chen, Effect of chemical stress on diffusion in a hollow cylinder, *J. Appl. Phys*., 2002, vol. 91, no. 12, pp. 9584–9590.

[44] H. Haftbaradaran, J. Song, W.A. Curtin, H. Gao, Continuum and atomistic models of strongly coupled diffusion, stress, and solute concentration, *J. Power Sources*, 2011, vol. 196, no. 1, pp. 361–370.

[45] Z. Erdélyi, G. Schmitz, Reactive diffusion and stresses in spherical geometry, *Acta Mater*., 2012, vol. 60, no. 4, pp. 1807–1817.

[46] M. Roussel, Z. Erdélyi, G. Schmitz, Reactive diffusion and stresses in nanowires or nanorods, *Acta Mater.*, 2017, vol. 131, pp. 315–322.

[47] B.L. Hess, J.J. Ague, Diffusion-induced stress in crystals: Implications for timescales of mountain building, *Lithos*, 2024, vol. 488–489, art. no. 107783.

[48] B.L. Hess, J.J. Ague, Modeling diffusion in ionic, crystalline solids with internal stress gradients, *Geochim. Cosmochim. Acta*, 2023, vol. 354, pp. 27–37.
[49] H. Yang, F. Fan, W. Liang, X. Guo, T. Zhu, S. Zhang, A chemo-mechanical model of lithiation in silicon, *J. Mech. Phys. Solids*, 2014, vol. 70, pp. 349–361.
[50] D. Clerici, F. Mocera, A. Somà, Analytical Solution for Coupled Diffusion Induced Stress Model for Lithium-Ion Battery, *Energies*, 2020, vol. 13, no.7, art. no. 1717.
[51] I.V. Belova, G.E. Murch, Thermal and diffusion-induced stresses in crystalline solids, *J. Appl. Phys.*, 1995, vol. 77, no. 1, pp. 127–134.
[52] R. Deshpande, Y.-T. Cheng, M.W. Verbrugge, Modeling diffusion-induced stress in nanowire electrode structures, *J. Power Sources*, 2010, vol. 195, no. 15, pp. 5081–5088.
[53] Z. Guo, T. Zhang, H. Hu, Y. Song, J. Zhang, Effects of Hydrostatic Stress and Concentration-Dependent Elastic Modulus on Diffusion-Induced Stresses in Cylindrical Li-Ion Batteries, *J. Appl. Mech.*, 2014, vol. 81, no. 3, art. no. 031013.
[54] J.L. Chu, S. Lee, The effect of chemical stresses on diffusion, *J. Appl. Phys.*, 1994, vol. 75, no. 6, pp. 2823–2829.
[55] Ya.S. Podstrigach, Diffusion theory of the anelasticity of metals, *J. Appl. Mech. Tech. Phys.*, 1965, vol. 6, pp. 56–60.
[56] F.C. Larche, J.W. Cahn, The effect of self-stress on diffusion in solids, *Acta Metall*., 1982, vol. 30, no. 10, pp. 1835–1845.
[57] F.C. Larche, J.W. Cahn, The Interactions of Composition and Stress in Crystalline Solids, *Journal of Research of the National Bureau of Standards*, 1984, vol. 89, no.6, pp. 467–500.
[58] F.C. Larche, J.W. Cahn, Thermochemical equilibrium of multiphase solid under stress, *Acta Metall*., 1987, vol. 26, no. 10, pp. 1579–1589.
[59] E.C. Aifantis, On the problem of diffusion in solids, *Acta Mech*., 1980, vol. 37, pp. 265–296.
[60] V.S. Eremeev, *Diffusion and Stresses*, Energoatomizdat, Moscow, 1984 (in Russian).
[61] J.-L. Grosseau-Poussard, B. Panicaud, S. Ben Afia, Modelling of stresses evolution in growing thermal oxides on metals. A methodology to identify the corresponding mechanical parameters, *Comput. Mater. Sci.*, 2013, vol. 71, pp. 47–55.
[62] Sh. Geng, K. Zhang, B. Zheng, Yu. Zhang, Effects of concentration-dependent modulus and external loads on Li-ion diffusion and stress distribution in a bilayer electrode, *Acta Mech*., 2024, vol. 235, pp. 191–201.
[63] Z. Cui, F. Gao, J. Qu, A finite deformation stress-dependent chemical potential and its applications to lithium ion batteries, *J. Mech. Phys. Solid.*, 2012, vol. 60, no. 7, pp. 1280–1295.
[64] J.L. Bouvard, D.K. Francis, M.A. Tschopp, E.B. Marin, D.J. Bammann, M.F. Horstemeyer, An internal state variable material model for predicting the time, thermomechanical, and stress state dependence of amorphous glassy polymers under large deformation, *Int. J. Plast*., 2013, vol. 42, pp. 168–193.
[65] X. Zhang, Q.J. Wang, H. Shen, A multi-field coupled mechanical-electric-magnetic-chemical-thermal (MEMCT) theory for material systems. *Comput. Method Appl. Mech. Eng.*, 2018, vol. 341, pp. 133–162.
[66] X. Zhang, Z. Zhong, A coupled theory for chemically active and deformable solids with mass diffusion and heat conduction, *J. Mech. Phys. Solids*, 2017, vol. 107, pp. 49–75.
[67] I. Gyarmati, *Non-equilibrium Thermodynamics. Field Theory and Variational Principles*, Springer-Verlag, Berlin, 1970.
[68] S.R. De Groot, P. Mazur, *Non-Equilibrium Thermodynamics*, Dover, New York, 1984
[69] R. Haase, *Thermodynamics of Irreversible Processes*, Dover, New York, 1969
[70] W. Liu, S. Shen, Coupled chemomechanical theory with strain gradient and surface effects. *Acta Mech*., 2018, vol. 229, pp. 133–147.
[71] G. Rambert, J. Grandidier, E. Aifantis, On the direct interactions between heat transfer, mass transport and chemical processes within gradient elasticity, *Eur. J. Mech. A*, 2007, vol. 26, no. 1, pp. 68–87.
[72] K.P. Frolova, E.N. Vilchevskaya, V.A. Polyanskiy, Yu.A. Yakovlev, Modeling the skin effect associated with hydrogen accumulation by means of the micropolar continuum, *Contin. Mech. Thermodyn*., 2021, vol. 33, pp. 697–711.
[73] P. Grigoreva, E.N. Vilchevskaya, W.H. Müller, Stress and Diffusion Assisted Chemical Reaction Front Kinetics in Cylindrical Structures, in: H. Altenbach, H. Irschik, V. Matveenko (Eds.), *Contributions to Advanced Dynamics and Continuum Mechanics. Advanced Structured Materials*, *vol 114*, Springer, Cham, 2019, pp 53–72.
[74] A.B. Freidin, I.K. Korolev, S.P. Aleshchenko, E.N. Vilchevskaya, Chemical affinity tensor and chemical reaction front propagation: theory and FE-simulations. *Int. J. Fract*., 2016, vol. 202, pp. 245–259.
[75] A.B. Freidin, I.K. Korolev, E.N. Vilchevskaya, Stress-assist chemical reactions front propagation in deformable solids, *Int. J. Eng. Sci*., 2014, vol. 83, pp. 57–75.
[76] A. Gusak, N. Storozhuk, Diffusion-Controlled Phase Transformations in Open Systems, in: A. Paul, S. Divinski (Eds.), *Handbook of Solid State Diffusion, vol. 2*, Elsevier, Amsterdam, 2017, pp. 37–100.
[77] R.-H. Fan, H.-L. Lu, K.-N. Sun, W.-X. Wang, X.-B Yi, Kinetics of thermite reaction in Al-Fe_2O_3 system, *Thermochim. Acta*, 2006, vol. 440, no. 2, pp. 129–131.
[78] H.A. Wriedt, The Al-O (Aluminum-Oxygen) system, *Bulletin of Alloy Phase Diagrams*, 1985, vol. 6, pp. 548–553.
[79] J.L. Murray, Fe–Al binary phase diagram, in: H. Baker (Ed.), *Alloy Phase Diagrams*, *vol. 3*, ASM International, Ohio, 1992, p. 54.
[80] O.K. Goldbeck, *Iron—binary phase diagrams*, Springer, Berlin, 1982
[81] S.V. Shukhardin, *Binary and Multicomponent Systems Based on Copper*, Nauka, Moscow, 1979 (in Russian).
[82] N.P. Lyakishev, Phase Diagrams of Binary Metal System, Metallurgiya, Moscow, 1997.
[83] Y. Nakamura, K. Sumiyama, H. Ezawa, Vapor quenched Fe-Ti alloys: Formation of amorphous phase, and metastable Ti_2Fe phase by aging, *Hyperfine Interact*., 1986, vol. 27, pp. 361–364.
[84] S.K. Misra, M. Kahrizi, K. Singh, N. Venkatramani, D. Bahadur, EPR, X-ray, and magnetization studies of metastable alloys Ti_2Fe, $Al_{40}Cu_{10}Mn_{25}Ge_{25}$ and $Al_{65}Cu_{20}Fe_{15}$ as prepared by mechanical alloying, *J. Magn. Magn. Mater*., 1995, vol. 150, no. 3, pp. 430-436.
[85] Y.-Ch. Lin, A.S. Shteinberg, P.J. McGinn, A.S. Mukasyan, Kinetics study in Ti-Fe_2O_3 system by electro-thermal explosion method, *Int. J. Therm. Sci*., 2014, vol. 84, pp. 369–378.

[86] B.A. Boley, J.H. Weiner, *Theory of Thermal Stresses*, Wiley, New York, 1960
[87] M. Anisimova, A. Knyazeva, Diffusion Interaction Model in Al-Fe_2O_3 System with Including the Formation of Intermetallic Phases, *Interfacial Phenom. Heat Transf.*, 2024, vol. 12, no. 1, pp. 75–88.
[88] V.N. Antsiferov, V.G. Gilev, The role of bulk and mass effects of reactions in reaction sintering processes, *Powder Metallurgy and Functional Coatings,* 2015, no. 4, pp. 9–20.
[89] L.N. Larikov, Mechanisms of reactive mutual diffusion (review), *Metallofiz. Noveishie Tekhnologii*, 1994, vol. 16, no. 9, pp. 3–27.
[90] V.I. Arkharov, On the kinetics of reaction diffusion in systems with several intermediate phases, *Physics of Metals and Metallography*, 1959, vol. 8, no. 2, pp. 193–204.

УДК 53.096+544.427+544.431

Напряжения в локальных объемах при реактивном спекании порошковой смеси Ti-Al-Fe-Fe_2O_3

А.Г. Князева, М.А. Анисимова

Институт физики прочности и материаловедения СО РАН, Академический пр., 2/4, Томск, 634055, Россия

Аннотация. Композиты на основе титана и алюминия привлекают внимание уже несколько десятилетий. Один из возможных способов создания таких композитов основан на реакционно (реактивном) спекании, которое подразумевает спекание с сопутствующими химическими реакциями, следствием которых является изменение фазового состава. В число реакций могут непосредственно входить те, которые приводят к образованию упрочняющей фазы. Весьма перспективными для использования в этом направлении являются смеси типа Ti-Al-Fe-Fe_2O_3, где источником оксида железа являются отходы металлообработки. Однако для многокомпонентных систем закономерности фазообразования, как и возникновения напряжений в диффузионной зоне, не очевидны и не одинаковы для всего объема реакционных смесей. В настоящей работе описываются общие идеи и методы моделирования реакционного спекания, а также дается обзор ситуаций, наиболее важных для фазообразования в выбранной смеси. Показано, что динамика роста фаз и напряжений может быть различной в разных локальных объемах с различными вариантами взаимодействия частиц друг с другом.

Ключевые слова: реактивная диффузия; рост фаз; напряжения